

CHAPTER III

An innovative suspension
bioreactor

Abstract

In tissue engineering, suspension culture techniques, aimed to guarantee a homogeneous three dimensional culture environment with enhanced mass transfer, have demonstrated their potentiality with respect to the traditional two-dimensional cell culture methods: they are currently used for low cost scalable cell expansion and long-term cell viability maintenance, for facilitating multicellular aggregate formation, for guiding differentiation of stem cells, and for the production of native-like three dimensional engineered tissues. However, the suspension devices currently adopted present some limitations, as the generation of non-physiological shear stresses and the expensive realization cost . With the aim to provide researchers with a yielding, versatile tool, we have developed an innovative low-cost perfusion bioreactor for culturing cells in suspension and low-shear conditions, without using electromechanical rotating systems. The peculiar geometric features of the culture chamber, designed with the support of a dedicated computational fluid dynamic study, allow the formation of buoyant vortices that guarantee the suspension condition within the culture chamber with low shear-stress values. In-house behavior/operating tests confirmed the suitability and the performances of the bioreactor, demonstrating the fittingness of the chamber isolation, and the establishment of suspension conditions with a homogeneous distribution of the samples within the culture chamber. Preliminary cellular tests assessed the suitability of the bioreactor in ensuring sterility and cell viability maintenance. This bioreactor is a compact system that easily fits into a standard cell incubator, representing a highly isolated dynamic cell culture setting, moreover it is characterized by a high versatility, since a wide range of flow patterns can be accomplished, permitting the adjustment of the dynamic culture parameters both to the types of cultured cells and to their developmental phase. In conclusion, the innovative developed bioreactor can be used as 1) model system, both for testing cytocompatibility and durability of cell microcarriers (e.g. hydrogel microspheres) and for investigating the influence of suspension condition on cells, with or without microcarriers, and as 2) expansion/aggregation/differentiation system, for *in vitro* three-dimensional cell culture.

Keywords: tissue engineering, bioreactor design, suspension condition, oxygenation, shear stress.

1. Introduction

Recently, suspension culture techniques, with or without cell microcarriers, have demonstrated their potentiality for low cost scalable cell expansion and long-term cell viability maintenance (Amit et al., 2010; Zweigerdt et al., 2011; Consolo et al., 2012; Olmer et al., 2012), for facilitating multicellular aggregate formation (Sen et al., 2001; Cameron et al., 2006; Wang et al., 2006), for guiding differentiation of stem cells (SCs) (Siti-Ismael et al., 2012), for preventing the dedifferentiation process that occurs under traditional two-dimensional (2D) cell culture conditions, maintaining specialized features of cells (Hammond and Hammond, 2001), and for the production of native-like three dimensional (3D) engineered tissues (Hwang et al., 2009; Yu et al., 2011).

To date, suspension condition is obtained with roller-bottles, stirred or rotating bioreactors.

The roller-bottle system, involved in advanced physiological and biochemical research on scale-up of anchorage-dependent mammalian cells and microorganisms, consists of cylindrical vessels that revolve slowly (between 5 and 60 revolutions per hour) which bathe the cells that are attached to the inner surface with medium. This system represents a very economical means for cultivating large quantities of anchorage-dependent cells using essentially the same culture techniques as with traditional cell culture flasks but with considerably less labor. In addition, besides providing larger surface areas for cell growth, culturing cells with roller-bottles has two advantages over static monolayer culture: firstly, the gentle agitation prevents gradients from forming within the medium that may adversely affect growth; secondly, cells spend most of their time covered by only a thin layer of medium, thus allowing for higher gas exchange (<http://www.sigmaaldrich.com/labware/labware-products.html?TablePage=9577881>). Some research groups have demonstrated that anchorage-dependent cells cultured within roller-bottles present higher proliferation rate (Polatnick and Bachrach, 1972; Yu et al., 2009; Andrade-Zaldívar et al., 2011), generating cell in large-scale, cutting down on the amount of laboratory manipulations, and saving both time and labor costs. Despite all these advantages, roller-bottles present some technological limitations and drawbacks. They impose severe mechanical stresses on the cultured constructs, with a mixing of fluid not well distributed especially in the axial direction. Moreover, due to the incomplete filling of the vessel, the air in the headspace creates turbulence and secondary bubble formation in the culture medium, which are both potent sources of extra shear and turbulence (Unger et al., 2000).

More recently, stirred bioreactors (or spinner flasks) were developed. Within these devices, a magnetic stirrer allows the mixing of the culture medium while the cultured constructs are fixed with respect to the moving fluid. Flow across the surface of the constructs results in eddies, turbulent instabilities consisting of clumps of fluid particles

that have a rotational structure superimposed on the mean linear motion of the fluid particles. They are associated with transitional and turbulent flow. It is via these eddies that fluid transport through the constructs is thought to be enhanced (Goldstein et al., 2001). Typically, spinner flasks are around 120 ml in volume (although much larger flasks of up to 8 liters have been used), and are run at 50-80 rpm (Freshney, 2000). Recent findings demonstrated that these 3D culture systems, based on both agitator design and agitation rate, as well as on the establishment of critical inoculum densities, provide an efficient *in vitro* environment for SC proliferation and differentiation, and could act as SC delivery microspheres for autologous tissue engineering (TE) (Fok and Zandstra, 2005; Cameron et al., 2006; Liu and Roy, 2006; Kehoe et al., 2010; Choi et al., 2011; Lee et al., 2011). Importantly, the use of these bioreactors enables the expansion of SCs in the absence of feeder layers or matrices, which will facilitate the adaptation of good manufacturing practice (GMP) standards to the development of SC therapies (Krawetz et al., 2010). However, due to both local turbulence and the high flow rates created between the vessel walls and the magnetic stirrers, stirred bioreactors impose non-physiological shear stresses on cultured constructs, therefore potentially inducing cell damage, and interfering with SC pluripotency. Moreover, this inhomogeneity in the shear field could limit the reproducibility of the culture process and the consequent interpretation of the results.

Starting from the need to minimize shear and turbulence in suspension cell cultures, NASA's Biotechnology Group developed an alternative bioreactor design, the rotating-wall vessel (RWV), with interesting and unique features for mammalian cell cultivation (Goodwin et al., 1993; Hammond and Hammond, 2001). This bioreactor exists in two different configurations, the High Aspect Ratio Vessel (HARV) and the Slow Turning Lateral Vessel (STLV) (Rodrigues et al., 2011). Both provide fluid dynamic operating principles characterized by 1) a permanent rotation of the culture chamber, the rotation speed of which is adjusted to produce a free-falling state, optimally reduced fluid shear and turbulence, and 3D spatial freedom; and 2) oxygenation by diffusion, excluding undissolved gases from the bioreactor (Wolf and Schwarz, 1991; 1992; Schwarz and Wolf, 1991; Goodwin et al., 1993). These technological solutions encourage a uniform growth of the tissues, and promote cellular interactions. Moreover, the RWV bioreactors protect fragile tissues from cracking because mechanical stresses are reduced, including shear stress, and the impact of the cells on the bioreactor walls is limited (Bilodeau and Mantovani, 2006). These bioreactors have been successfully used for osteogenic (Granet et al., 1998; Qiu et al., 1999; Turhani et al., 2005; Song et al., 2006) and cardiomyogenic (E et al., 2006) differentiation, and cartilage TE (Marolt et al., 2006). However, rotating bioreactors are expensive devices due to their complex technological solutions, and scaling up processes may be complex (Hammond and Hammond, 2001; Rodrigues et al., 2011).

In order to overcome the previously presented limitations, we have developed an innovative multipurpose low-cost perfusion bioreactor (patented, Falvo D'urso Labate et

al., 2012) able to establish a biochemical and hydrodynamic environment suitable for maintaining specimen of different dimensions (i.e., cells, microspheres etc.) in suspension conditions within a 3D culture environment. The peculiar geometric features of the bioreactor assure the possibility for buoyant vortices to be generate within the culture chamber, without using electromechanical rotating systems and avoiding shear stress values critical for the cells, guaranteeing a suitable and homogeneous distribution of oxygen and nutrients. In-house behavior/operating tests confirmed the suitability and the performances of the bioreactor, demonstrating the fittingness of the chamber isolation, and the establishment of suspension conditions with a homogeneous distribution of the samples within the culture chamber. Preliminary cellular tests assessed the suitability of the bioreactor in ensuring sterility and cell viability maintenance. In conclusion, the innovative developed bioreactor can be used as 1) model system, both for testing cytocompatibility and durability of cell microcarriers (e.g. hydrogel microspheres) and for investigating the influence of suspension condition on cells, with or without microcarriers, and as 2) expansion/aggregation/differentiation system, for *in vitro* 3D cell culture.

2. Materials and Methods

2.1 Device requirements

The bioreactor was designed and developed in order to guarantee a suitable biochemical and hydrodynamic 3D culture environment for maintaining specimen of different dimensions (i.e., cells, microspheres etc.) in suspension conditions with enhanced mass transfer and low shear stress.

Within the bioreactor, suspension is obtained due to peculiar geometric features which assure the possibility for buoyant vortices to be generate, allowing the device to create suspension conditions, and to be employed with several constructs and for different applications. In order to assure full compatibility with GMP procedures, the bioreactor was developed for satisfying the following requirements:

- cytocompatibility and corrosion-resistance of all the materials in contact with culture medium;
- ease of sterilization and sterility maintenance;
- ease of use (assembly in sterile conditions under a laminar flow hood, cleaning, use for non-trained staff);
- small dimensions, suitable for positioning in a cell culture incubator;
- no medium stagnation during exchange operations.

2.2 Architectural design

Key constitutive elements of the bioreactor are (Figure III.1):

- a transparent, sealable and sterile **culture chamber** where cells, with or without microcarriers, and culture medium are housed during the experiments;
- a **perfusion subsystem** constituted by a medium reservoir, a peristaltic pump, and oxygen permeable tubes (oxygenation module), that is designed to maintain the suspension environment.

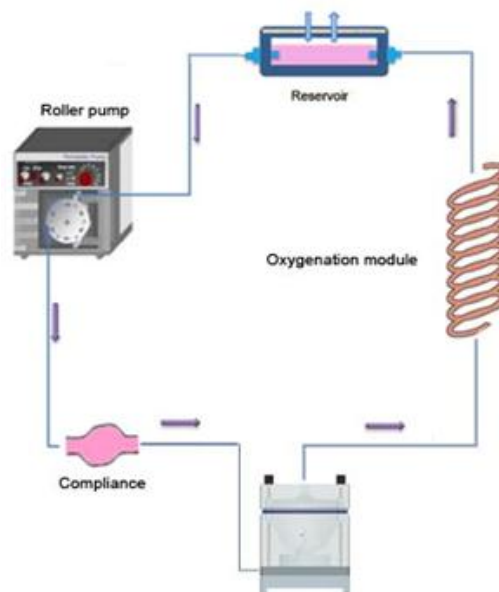


Figure III.1. Architectural design of bioreactor constituted of: a medium reservoir; a peristaltic pump; a culture chamber; and oxygen permeable tubes.

Pumped by a peristaltic pump the culture medium enters from the base, opens the check valve, and pervades the culture chamber, flowing out from the top (Figure III.2).

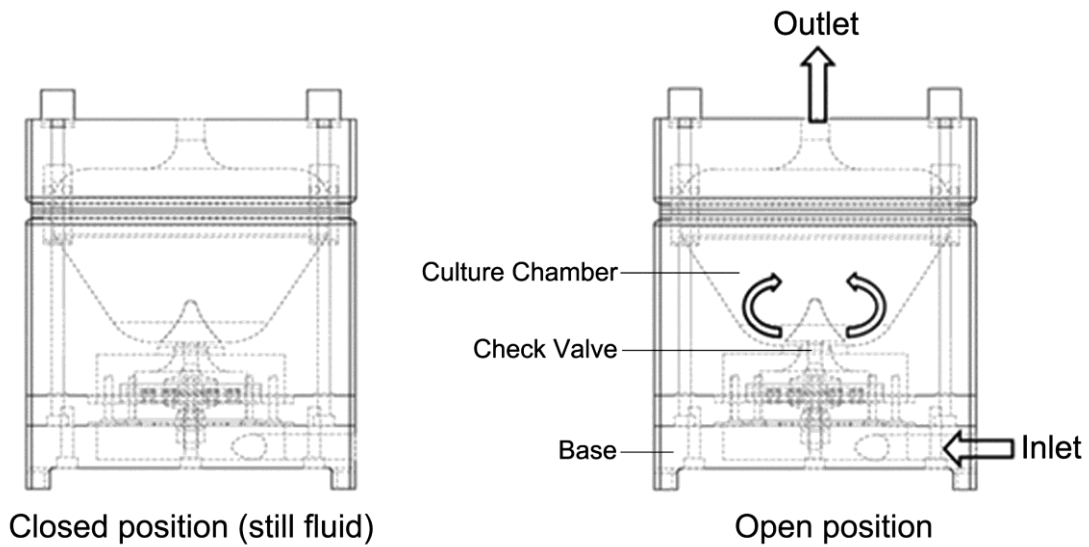


Figure III.2. Bioreactor constructive drawing. Flow direction/movement is highlighted. Configuration with check valve in the closed position (left). Configuration with check valve in the open position (right).

During the experiment, the culture chamber, the fresh media reservoir, and a portion of the oxygen-permeable tubes are positioned within the incubator. The peristaltic pump is positioned outside to protect it from the high humidity (95% - 37°C) that characterizes the internal environment of the incubator (Figure III.3). Depending on the model of incubator, we tested two configurations of the bioreactor within the incubator, i.e., whether it presents (Figure III.3 right panel) or not (Figure III.3 left panel) an exit hole.

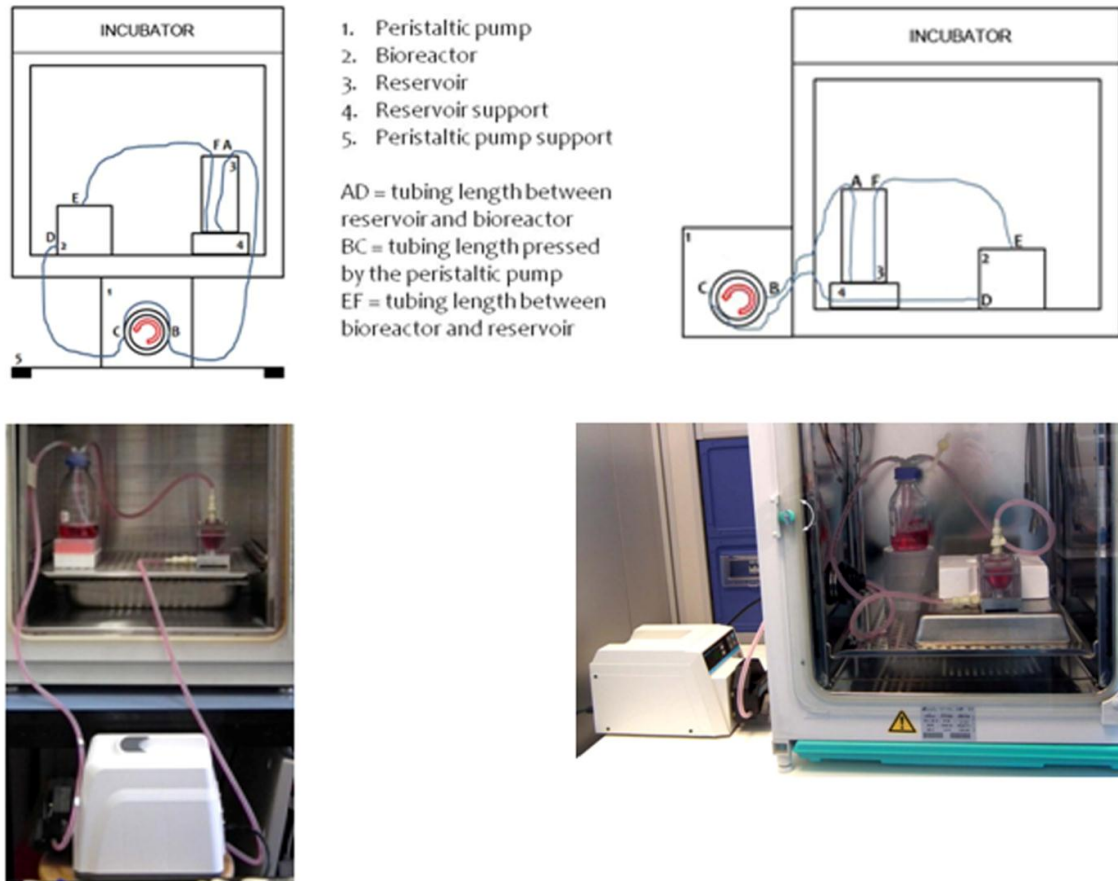


Figure III.3. Bioreactor set-up within the incubator in the two possible configurations. Schematic drawing (top) and picture (bottom) of the bioreactor set-up within a incubator without an exit hole (left panel). Schematic drawing (top) and picture (bottom) of the bioreactor set-up within a incubator with an exit hole (right panel). The legend refers to both configurations.

2.3 Bioreactor constitutive elements

2.3.1 Culture chamber

The bioreactor culture chamber (component 5 in Figure III.4b), where cells are cultured, has been designed to be a sterile and cytocompatible environment. It has been manufactured through material removal by a micrometrical controlled cutter from a polycarbonate (PC) bulk piece, a choice that guarantees biocompatibility and easier sterilization by autoclave. The inner dimensions are approximately $95 \times 70 \times 70 \text{ mm}^3$ with a working volume of 75 ml. The geometric features of the bioreactor culture chamber have been designed with the final goal to establish the formation of buoyant vortices, and therefore the generation of suspension condition. Moreover, rounded edges were designed in order to avoid stagnation points and discontinuities, fissures, interstices, holes, which are preferable targets for microbial contamination. Within the culture chamber are located 1) a check valve for guarantying the unidirectionality of the flow (component 6 in Figure III.4b), and 2) a

filter, for preventing accidental outputs of cells or constructs during the recirculation of the culture medium (component 4 in Figure III.4b).

Figure III.4b shows a detailed view of the bioreactor components.

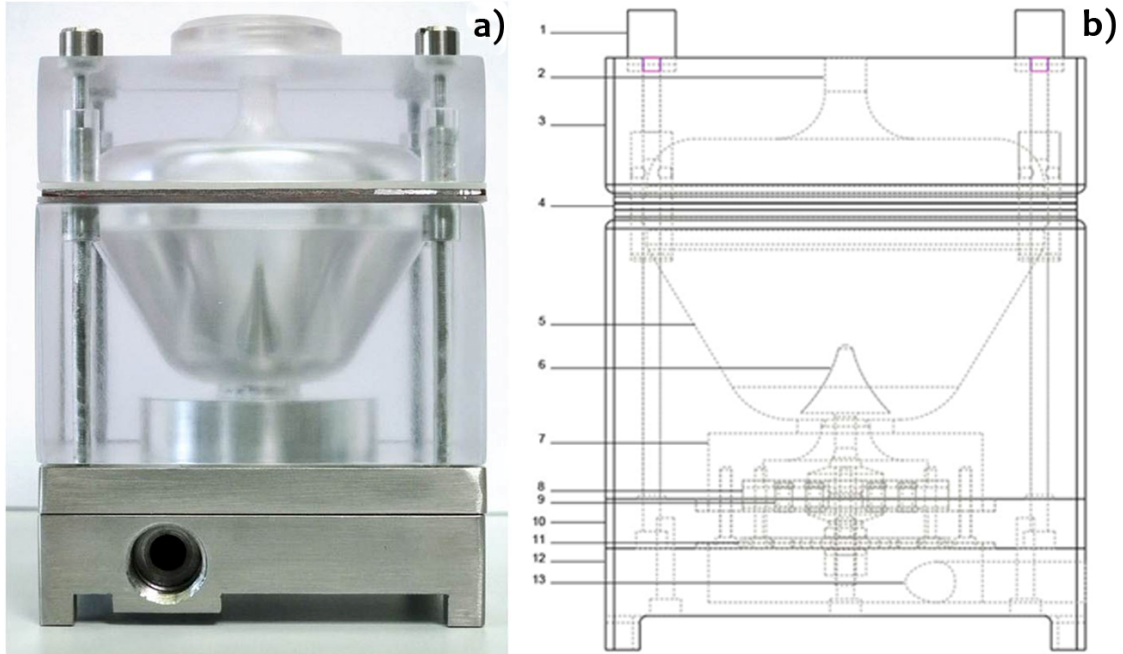


Figure III.4. Bioreactor. a) Picture of the entire device. b) CAD design of the bioreactor components: (1) thumb screw, (2) flow outlet, (3) lid, (4) filter, (5) culture chamber, (6) check valve, (7) membrane holder 1, (8) membrane, (9) bushing, (10) membrane holder 2, (11) perforated plate (collimator), (12) base, (13) flow inlet.

Check valve

The innovative check valve (Figure III.5) has been designed for guarantying the unidirectional flow of the culture medium within the circuit. The valve motion from the closed to the open position and *vice versa* is vertical and it is obtained by means of a moving silicone membrane.

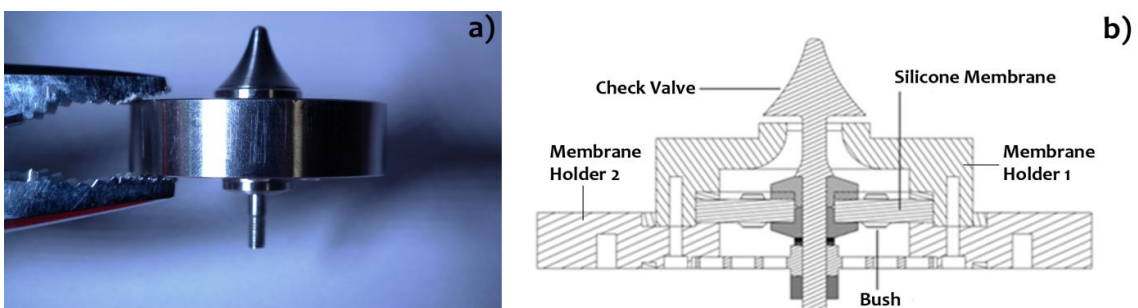


Figure III.5. Check valve. a) Picture of the check valve without the membrane holder 2. b) Check valve CAD design.

The flow of the culture medium within the device is achieved by production of over pressures in the valve chamber, with respect to the culture chamber: the medium flows only when the transvalvular pressure difference overcomes the cracking pressure of the valve. The silicone membrane, with a thickness of 2 or 3 mm depending on the rigidity which is desired for the system, is designed with six holes, each one of them housing a bushing that can be open or closed in order to modulate the proper operating transvalvular pressure (Figure III.6).



Figure III.6. Picture of the silicone membrane. a) Lateral view. b) Three possible configurations; from the left: 2, 4 or 6 open holes, respectively. c) Silicone membrane assembled with the check valve system.

Filter

The PolyVinylidene Fluoride filter (PVDF - Durapore[®] Millipore, free passage diameter = 5 μm – porosity = 80%) has been designed in order to prevent accidental outputs of cells or constructs during the recirculation of the culture medium. In addition to the PVDF filter, the entire filter set-up has been designed considering also the insertion of 3 silicone washers and one AISI 316L stainless steel grate (Figure III.7a-f).

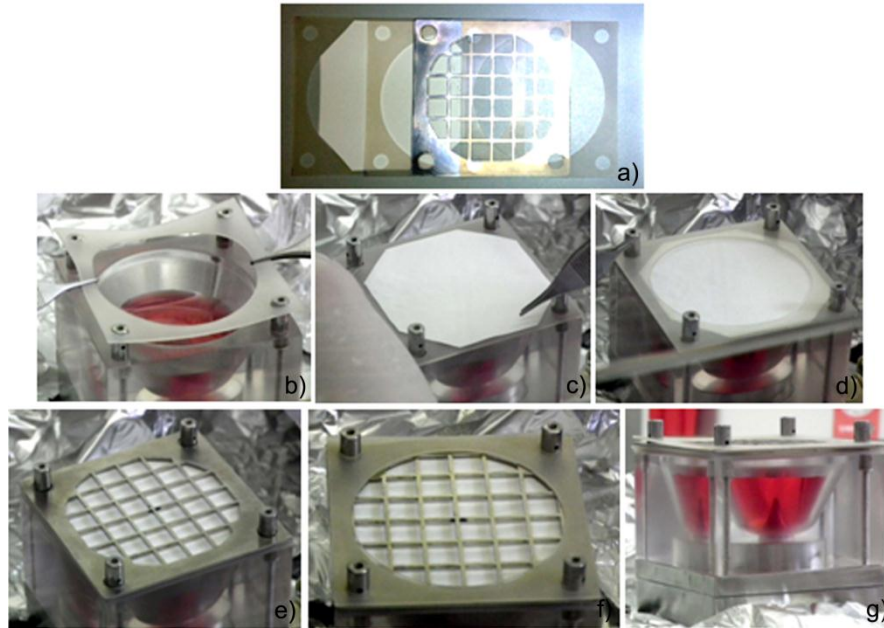


Figure III.7. Bioreactor filter set-up. a) Filter components. b) Insertion of the first silicone washer. c) Insertion and positioning of the PVDF filter. d) insertion of the second silicone washer. e) insertion of the AISI 316L stainless steel. f) Insertion of the third silicone washer. g) completed filter set-up.

The first two silicone washers, positioned before and after the PVDF filter, allow to maintain the correct positioning of the filter, and to prevent leakage of the medium (Figure III.7b-d). The AISI 316L stainless steel grate, positioned after the second silicone washer, ensures greater rigidity of the PVDF filter, avoiding sudden breakage due to accidental air bubble formation or pressure increases within the culture chamber (Figure III.7e). Finally, the last silicone washer positioned between the grate and the lid, guarantees the tightness of the coupling, and allows to avoid direct contact between the AISI 316L stainless steel of the grate and the PC of the lid, potentially causing damages of the material (Figure III.7f).

2.3.2 Perfusion subsystem

The perfusion subsystem (Figure III.8) is composed of a medium reservoir, a peristaltic pump, quick-disconnected couplings, and oxygen-permeable tubes.

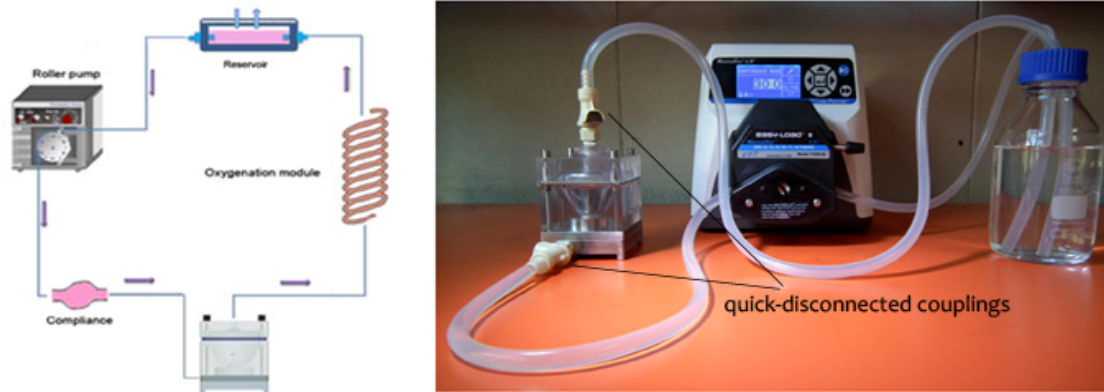


Figure III.8. Bioreactor perfusion subsystem set-up.

Medium reservoir

The role played by the reservoir is dual: it contains sterile medium for cell feeding, and it enhances mass transfer to provide oxygenated media (it is a free-surface reservoir) (Figure III.9).

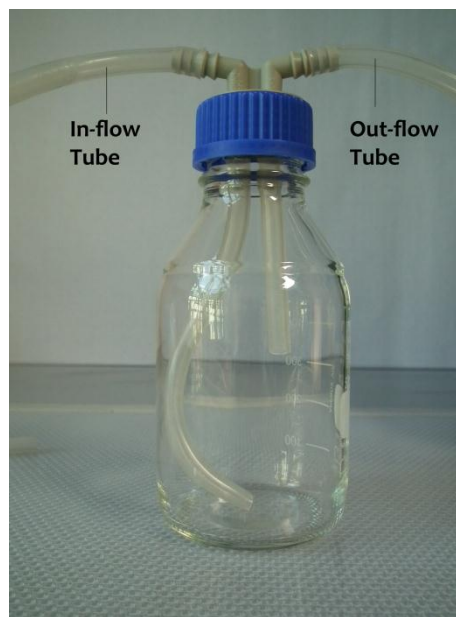


Figure III.9. Picture of the medium reservoir with the in-flow and out-flow tube.

Pump

A peristaltic pump has been chosen (Masterflex L/S® RX-07551 – 00) to assure recirculation. Pump features are summarized in Table III.1:

Table III.1. Technical features of the Masterflex L/S® RX-07551 – 00 pump.

Flow rate values	0.006 - 3400 ml/min
VAC	90/260
rpm	0.1 - 600
Speed control	precision digital \pm 0.1%
Operating temperature	0 - 40°C
Drive dimensions	25.4 cm x 21.6 cm x 21.6 cm (10" x 8.5" x 8.5")
motor	75 watts, 1/10 hp

Couplings

Cole-Parmer quick-disconnect couplings able to process the fluidic circulation in the system and to ensure unidirectionality to the flow have been chosen (Figure III.10). Coupling features are summarized in Table III.2.

Table III.2. Technical features of the Cole-Parmer quick-disconnect couplings.

Body material	Acetal
Seal material	Ethylene Propylene Rubber (EPR)
Spring and latch material	316 Stainless Steel
Max vacuum	28" Hg
Max temperature	71°C
Max pressure at 21°C	100 psi



Figure III.10. Cole-Parmer quick-disconnected couplings.

Tubing

The oxygenation and partially the hydraulic compliance are assured by the Masterflex BioPharm Platinum-Cured Silicone Pump Tubing (Hose barb 1/4", ID 6.4 mm), retaining the following features shown in Table III.3:

Table III.3. Technical features of the Masterflex BioPharm Platinum-Cured Silicone Pump Tubing.

Material	Tygon 3350 silicone, platinum-cured
Operating temperature	-60 to 232°C
Methods of sterilization	Ethylene oxide, gamma irradiation, or autoclave for 30 min, 15 psi

Permeability properties to CO₂, H₂, O₂ and N₂ are summarized in Table III.4.

Table III.4. Permeability properties of Masterflex BioPharm Platinum-Cured Silicone Pump Tubing.

Permeability (approx) at 25°C			
<i>Units: $\left\{ \frac{cc - mm}{sec - cm^2 - cmhg} \right\} \times 10^{-10}$</i>			
CO ₂	H ₂	O ₂	N ₂
20,132	6579	7961	2763

In *Appendix III.A*, at the end of the chapter, the sizing of the perfusion subsystem with a detailed description of the methods and the results obtained, is reported considering two different cases: 1) a fixed number of cells, considering neonatal rat cardiomyocytes (CMs) and 2) a variable number of cells due to proliferation, modeling mesenchymal stem cells (MSCs).

2.4 Computational fluid dynamic study

Computational fluid dynamic (CFD) multiphysics simulations were performed to identify the optimal design and proper operating conditions that optimize mass transport, and to study the construct-medium interaction.

A customized commercial software based on finite volume technique (FLUENT, ANSYS Inc., USA) was used. Previously, axial symmetric single phase computational simulations were performed to identify the optimal wall shape promoting the generation of buoyant vortices. The culture medium (density=1006.5 kg/m³, viscosity=0.001 kg/(m·s)) was simulated as Newtonian fluid. Afterwards, the 3D fluid domain within the culture chamber was discretized with approximately 2x10⁶ tetrahedral cells (Figure III.11), and 3D multiphase simulations were performed (time step = 2 ms), considering culture medium as primary phase and hydrogel microspheres (density=1118 kg/m³, viscosity=0.001 kg/(m·s), diameter=200 μm) as secondary phase.

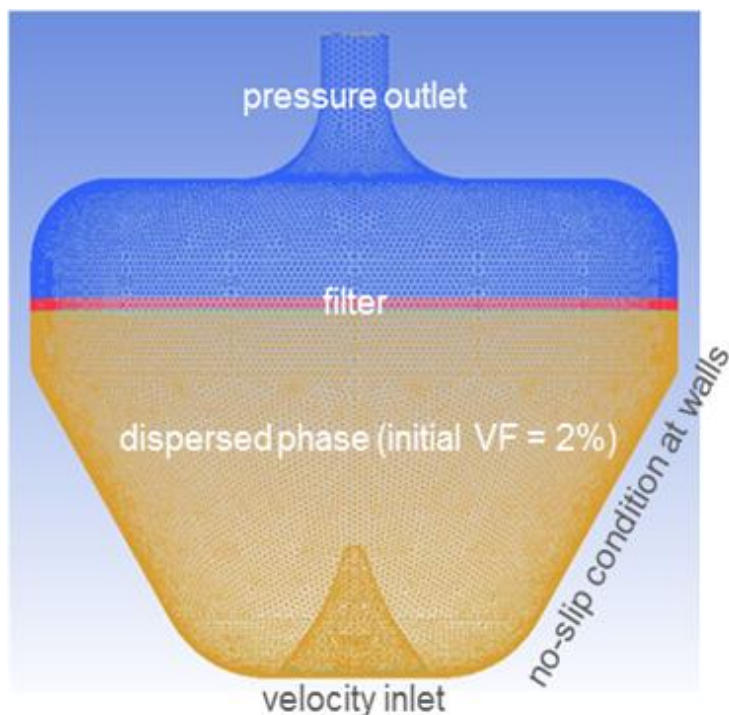


Figure III.11. Discretization of the 3D fluid domain with imposed conditions.

The concomitant presence of culture medium and microspheres was modeled using the Eulerian–Eulerian Multiphase Model, which allows to describe mixtures of multiple separated yet interacting phases. As initial condition, a volume fraction (VF) of microspheres equal to 2% was uniformly set in the lower region of the bioreactor. The filter was modeled as porous medium, impermeable to the microspheres phase. CFD simulations were carried out varying the inlet velocity of the culture medium (laminar flow condition). At the wall, no slip conditions were imposed.

2.5 Tests

2.5.1 In-house factory tests

Preliminary in house/behavior tests were conducted to investigate suitability and performances of each component of the bioreactor. In particular, tests 1) to understand if the bioreactor was able to withstand the stresses due to the passage of the fluid, 2) to investigate the ability to generate buoyant vortices, with the consequent establishment of suspension condition, and 3) to find out the proper bioreactor configuration that allows a homogeneous distribution of the cells or constructs within the culture chamber, were performed. As preliminary test, to simulate the presence of constructs within the culture chamber, injectable thermoreversible polyurethane (PU) microspheres (with a diameter equal to 500 μm after swelling) were used.

2.5.2 Preliminary cellular tests

With the aim to verify the suitability of the device to be used in cardiac TE, a preliminary test of dynamic cell culture was performed by the Group of Professor Quaini, Department of Internal Medicine and Biomedical Sciences, Section of Internal Medicine, University of Parma, Italy.

Enhanced Green Fluorescent Protein Cardiac Progenitor Cells (EGFP^{POS} CPCs) isolated from adult EGFP rat hearts (for detailed procedure see Beltrami et al., 2003), were seeded on gelatin/gellan microspheres with an average diameter of 125÷300 or 350÷450 µm, respectively. Gelatin/Gellan microspheres functionalized with Insuline-like Growth Factor 1 (IGF-1, 0.25µg/mg) with diameter less than 90 µm were also tested. Dynamic culture of EGFP^{POS} CPCs alone was used as control.

Cells were seeded on cardiac injectable microspheres at the concentration of 10⁵cells/100µl and statically cultured for 48 h in complete growth medium (IMDM (Sigma, Italy), 1% P/S (Sigma, Italy), 1% I/T/S (Sigma, Italy), 10% FBS (Sigma, Italy)) to promote cell-microsphere adhesion. Analysis by inverted and fluorescence microscope (Leica DMI6000B) was performed immediately after mixing cell to microspheres to document efficiency of suspension.

After 48 hours of static culture, the adhesion of the cells to the biomaterials was assessed employing inverted and fluorescence microscope. After visualization, the suspension of EGFP^{POS} CPCs and microspheres was inserted within the culture chamber for a total number of cells equal to 6X10⁵, and in detail for a cell density of 1.2 X10⁴ cells/ml, and cultured for further 24 h in dynamic conditions (flow rate 5 ml/min).

After 24h of dynamic culture cells and microspheres were rescued from the culture chamber, re-suspended in fresh growth medium, seeded in a “Ultra Low-Attachment” 96 well plate (Corning, USA) to avoid adhesion and analyzed with optical and fluorescence microscopes to assess the conjugation between EGFP^{POS} CPCs and microspheres. In order to verify if the presence of cells was limited to the culture chamber, the culture medium was also collected from reservoir, tubes, lid and base. Moreover, the filter was fixed with paraformaldehyde (PFA) 4% for 30 minutes and then stained with DAPI (4',6-diamidino-2-phenylindole, Sigma, Italy) for 15 minutes at room temperature in order to verify the presence of cells on its surface. Photomicrographs of EGFP^{POS} CPCs collected from the culture chamber were taken and then analyzed by a software for image analysis (Image Pro-plus 4.0, Media Cybernetics, Inc., USA), to quantify cell persistence, adhesion and distribution on cardiac injectable prototypes.

After image analysis, EGFP^{POS} CPC – microsphere suspension was re-seeded on “Normal-Attachment”96-well (Corning, USA), and cultured for 5 days in static conditions to verify cell survival and proliferation.

The quantitative analysis of cell adhesion to microspheres after 24 h of dynamic culture and after 5 days in static condition was performed evaluating the fractional area occupied by EGFP^{POS} CPCs. Briefly, green fluorescence emission and its intensity, expressed as Integrated Optical Density (IOD), were computed using a software for image analysis (Image Pro-plus 4.0, Media Cybernetics, Inc., USA).

All images were acquired with precalibrated gain and exposure time. Aspecific fluorescence was carried out by merging the emission signals from different excitation lengths on the same microscopic field.

3. Results

3.1 Computational fluid dynamic study

Results of CFD simulations performed for assisting the bioreactor design, for studying the microspheres-medium interaction, and for identifying the operating conditions that optimize mass transport were performed are summarized in Figure III.12.

This figure shows contour map of microsphere VF with superimposed microsphere velocity vector field obtained from the 3D simulations (flow rate = 90 ml/min).

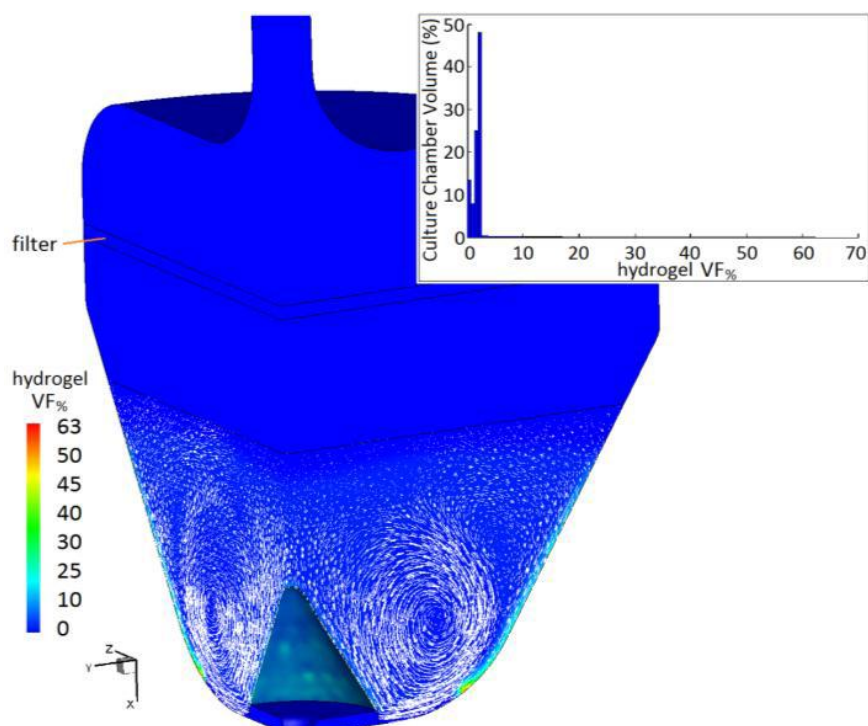


Figure III.12. Map of microsphere VF superimposed to microsphere velocity vector field. Inset: distribution of microsphere VF within the culture chamber volume. The microsphere VF peak value of 63% is the packing limit value for the microspheres, as well indicated, but never attained.

A buoyant toroidal vortex develops in the lower region of the culture chamber, counterbalancing the gravity force acting on microspheres and maintaining them in suspension (no microsphere sedimentation was observed). Near to the outer wall, a smaller second toroidal vortex (red arrow) is generated, which could play the beneficial role of enhancing the mixing of floating microspheres. The maintenance of microsphere VF values close to the initial value (2%) indicates that detrimental microsphere/microsphere collisions are avoided. This result is also confirmed by the analysis of the distribution of the microsphere VF within the lower part of the flow chamber (i.e., where microspheres are present): the inset in Figure III.12 shows that (1) about the 95% of the microspheres is subjected to low packing levels (VF lower than 3.9%), and (2) only the 2.7% of the microspheres is subjected to packing greater than VF=10%. These results are a further demonstration that, within the bioreactor, microsphere suspension is promoted while sedimentation is avoided. As for possible cell damage, it was found that in the lower part of the culture chamber the 95% of the suspended microspheres is subjected to shear stress values lower than 17 mPa equal to 0,17 dyn/cm². This finding confirms that there is no risk of mechanical damage to cultured cells when suspension condition is generated into the bioreactor (Isu et al., 2013).

Findings from CFD simulations are in agreement with the experimental results presented in the following sections.

3.2 Tests

3.2.1 In-house factory tests

Initially, to demonstrate the suitability of the device, the generation of buoyant vortices, and the consequent establishment of suspension condition, in house behavior/operating tests were performed.

The first test was dedicated to verify the suitability of the bioreactor to withstand the hydrodynamic pressures developing within the culture chamber due to the perfusions subsystem. Therefore, proceeding step by step, the flow rate was increased of 10 ml/min at each step, starting from 10 ml/min and reaching the final value of 250 ml/min. With these tests it has been demonstrated that the bioreactor responds well to any stress imposed by the flow rate. Moreover, no losses have been observed, and disassembling the bioreactor no abnormalities in the control system of the check valve have been noticed. The test certificated the fittingness of chamber isolation, and the ability of the bioreactor to withstand even at high flow rates.

The second test was dedicated to assess the formation of buoyant vortices and consequent suspension conditions within the culture chamber, finding out the proper bioreactor configuration that allows a homogeneous distribution of the cells or constructs

within the culture chamber. Findings obtained confirmed by visual inspection that, using the two possible configurations reported in Figure III.13, injectable thermoreversible PU microspheres were homogenously distributed within the culture chamber, no microsphere sedimentation occurs, and no microspheres reached the filter (Figure III.14).

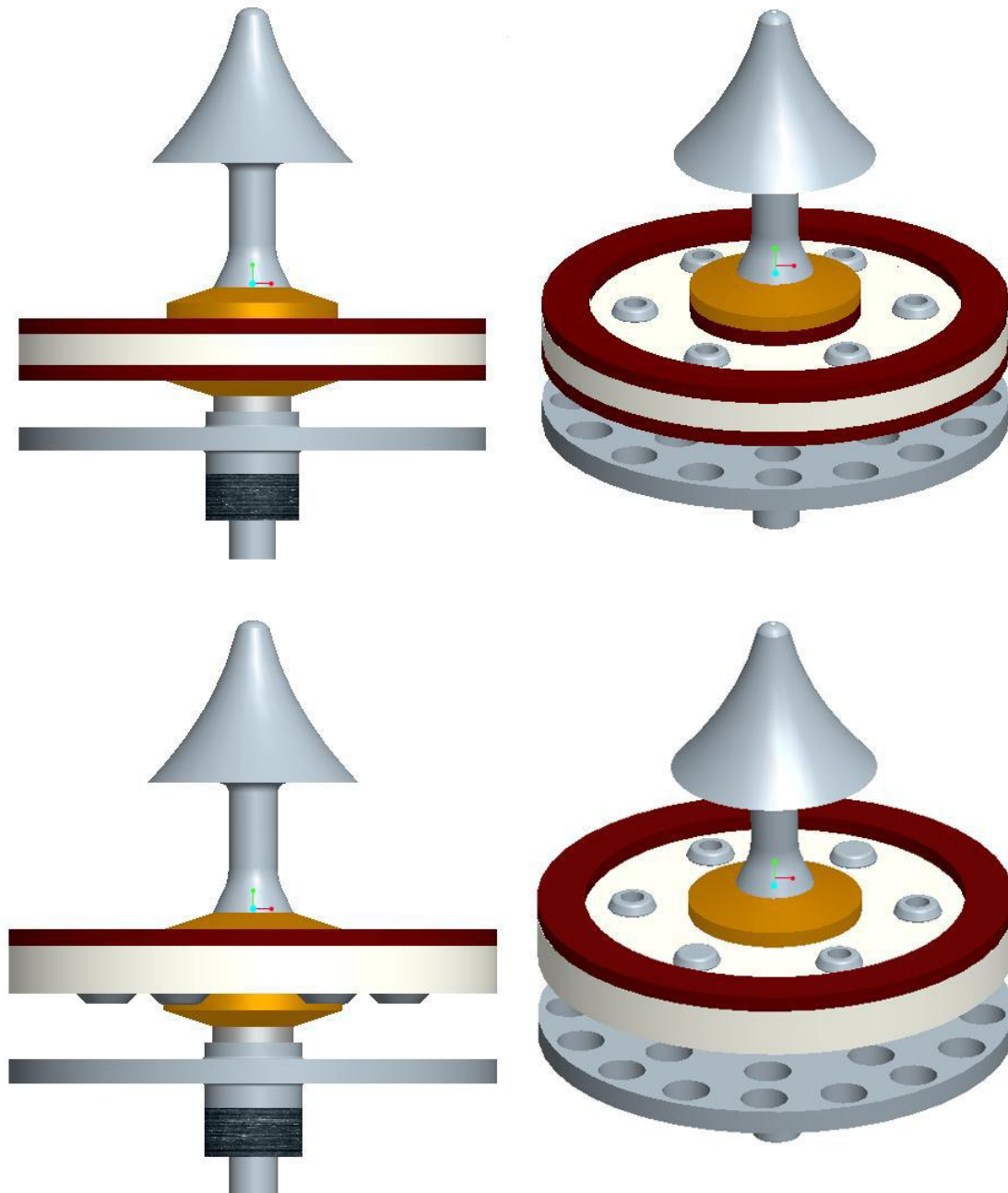


Figure III.13. CAD design of the bioreactor configurations that allow a homogenous distribution of samples within the culture chamber. Configuration with the 2mm thickness silicone membrane (top). Configuration with the 2mm thickness silicone membrane (bottom).

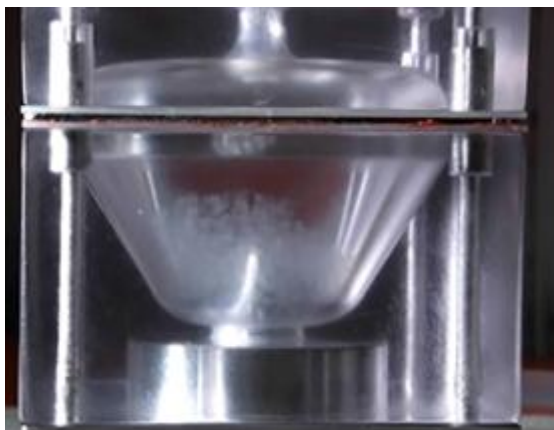


Figure III.14. Picture of the injectable thermoreversible PU microspheres homogeneously distributed within the culture chamber.

In detail, findings from in-house behaviour tests and CFD simulations have demonstrated that the maintenance of adequate suspension conditions is achieved through the attainment of a dynamic balance among the different forces acting simultaneously. The result of the balance between hydrodynamic and gravitational forces is the achievement of suspension for cultured cells or constructs, within a dynamic environment in which the shear stress values acting on the cells are lower respect to the critical values and the nutrient supply to the cultured cells is maximized.

The proper combination (1) of the fluid dynamic conditions establishing at the inlet of the chamber with (2) the shape of the side walls of the chamber itself give rise to flow separation, with the consequent formation of stationary buoyant vortices and of hydrodynamic forces the resultant of which balances the gravitational force, thus avoiding the sedimentation of cultured specimen at the bottom of the culture chamber. In detail, the suspension condition results from a net sum of all forces present equalling zero, not from an absence of gravity (Klaus, 2001). Gravitational and hydrodynamic forces, including buoyant and drag forces which result from the operating chamber in the gravitational field, combine simultaneously to produce a “suspension” condition for the immersed particles. In this way particles experience an average near zero gravitational force, thereby leading to what has been described as the “simulated microgravity” condition. Furthermore, the buoyant vortex assures proper mixing within the chamber and hence oxygen uptake to the cells.

The fluid (i.e., the culture medium) is mixed within a laminar flow environment and potentially damaging cell due to bead-fluid friction and bead-bead collisions is minimized in suspension conditions, conversely to what has been reported for dynamic bioreactors based on the agitation/stirring mechanism, where the onset of turbulences in the fluid flow typically occurs.

This design philosophy allows to not incorporate rotating components within the device.

3.2.2 Preliminary cellular tests

Preliminary cellular tests demonstrated that all the materials, that can be sterilized by autoclave before setting up the experiment, are highly cytocompatible and corrosion resistant. The set up procedure can subsequently be performed under a laminar flow hood in accordance with the GMP rules, maintaining the sterility of the culture chamber. Thanks to the limited number of components and to the bioreactor organization, the operations that need to be conducted under laminar flow are: (1) closure of the base; (2) priming and start of the peristaltic pump; (3) injection of the cells; (4) positioning of the filter; (5) insertion of the lid; and (6) closure of the perfusion circuit. All of them can be quickly and easily performed maintaining the sterility of the culture chamber and of the biological samples during the entire experiment. Moreover, these tests confirmed that, throughout the duration of the experiment, the bioreactor has proved to be a reliable, autonomous and safe device, able to guarantee the sterility and the viability of the cell culture. The culture chamber, which proved to be extremely comfortable in handling, showed no sign of microbial contamination; medium reservoir and permeable tube provided the necessary oxygen supply to cultured cells; and no cells were found on the PVDF filter or within the medium collected from the medium reservoir, lid, tubes, and base of the bioreactor, certifying the fittingness of chamber isolation.

In detail, results from preliminary tests demonstrated initially the cell-gelatin/gellan microsphere conjugation (Figure III.15).

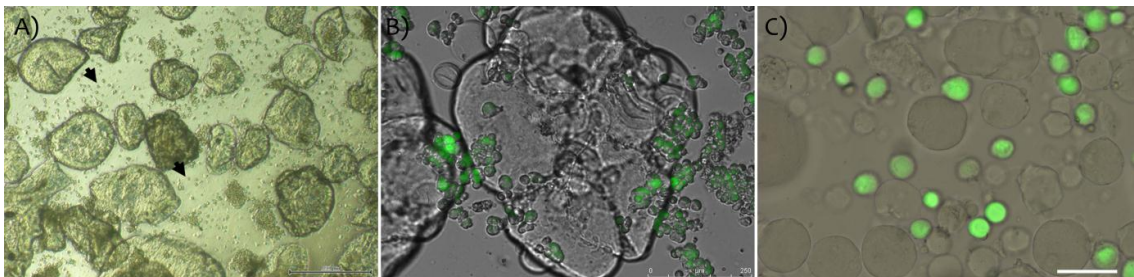


Figure III.15. Cell-microsphere constructs before static culture. A) CPCs (black arrows) and microspheres (125 ÷ 300 µm) in suspension. Scale bar 200 µm. B) EGFP^{POS} CPCs (green fluorescence) and microspheres (350 ÷ 450µm) in suspension. Scale bar 250 µm. C) EGFP^{POS} CPCs (green fluorescence) and microspheres functionalized with IGF-1 (d₉₀) in suspension. Scale bar 50 µm.

It is possible to observe a homogeneous distribution of the two components, with differences between the different type of microspheres. Microspheres with a diameter ranging from 125 to 300 µm are better separated from each other (Figure III.15A), whereas microspheres with a diameter ranging from 350 to 450 µm tend to aggregate (Figure III.15B). On the other hand, microspheres functionalized with IGF-1 (d₉₀) and EGFP^{POS} CPCs, suspended in growth medium, are individually and equally distributed (Figure III.15C).

After 48 hours of static culture, cells adhered to the surface of $125 \div 300 \mu\text{m}$ microspheres mainly as clusters (Figure III.16). On the other hand, EGFP^{POS} CPCs were conjugated to $350 \div 450 \mu\text{m}$ microspheres mainly as individual cells laying the cytoplasm over microsphere surface (Figure III.17).

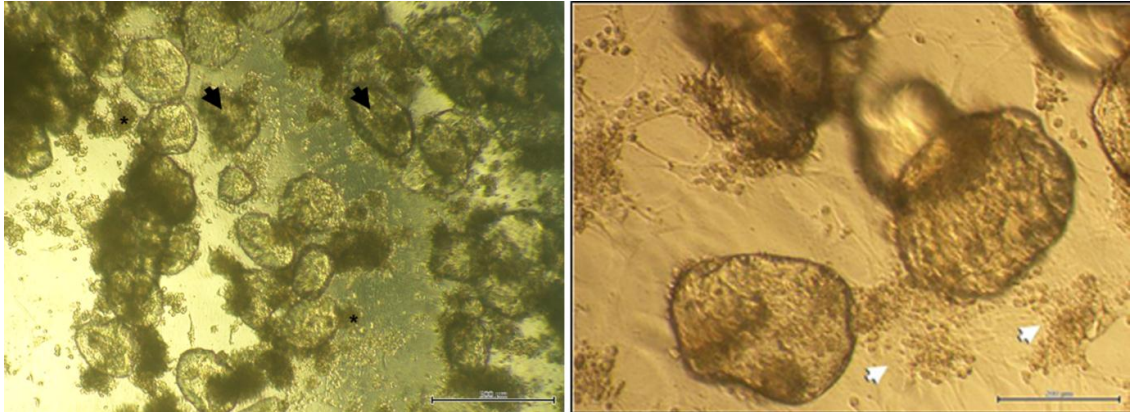


Figure III.16. CPCs seeded on $125 \div 300 \mu\text{m}$ microspheres after 48h of culture in static condition. Black arrows indicate cells adhered to microspheres and asterisks indicate cell clusters; white arrows point out to single cells which adhered to the bottom of the dish. Scale bars: $500 \mu\text{m}$ (left) and $200 \mu\text{m}$ (right).

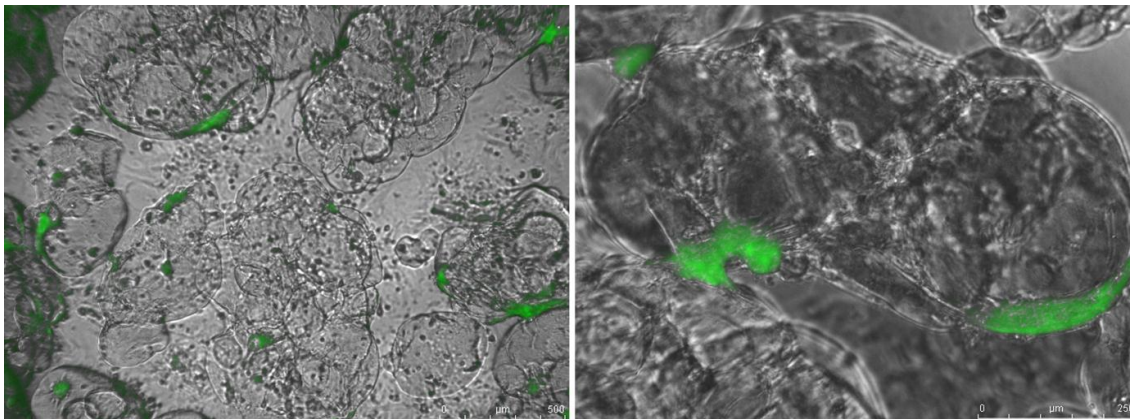


Figure III.17. CPCs seeded on $350 \div 450 \mu\text{m}$ microspheres after 48h of culture in static condition. Green fluorescence corresponds to cells adhered to microspheres at different magnifications. Scale bars: $500 \mu\text{m}$ (left) and $250 \mu\text{m}$ (right).

EGFP^{POS} CPCs adhere to microspheres functionalized with IGF-1 mainly as individual cells. Moreover, the presence of microspheres with altered morphology, probably due to an early degradation process, was observed (Figure III.18).

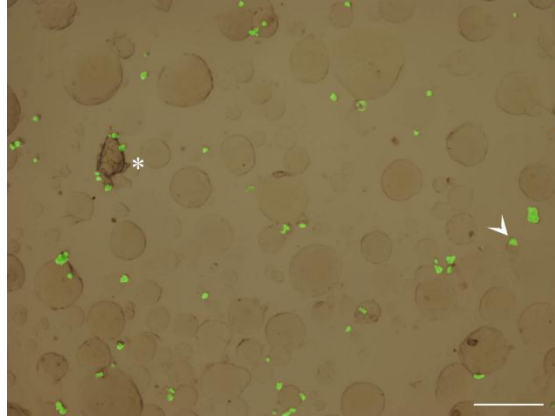


Figure III.18. EGFP^{pos} CPCs (green fluorescence) seeded on microspheres functionalized with IGF-1 after 48h of culture in static condition. White arrowhead indicates a single cell adhering to microsphere and asterisk indicates microsphere with altered shape. Scale bar 200 μ m.

Results after 24 hours of dynamic culture are described below.

- **Gelatin/gellan injectable microspheres (diameter 125÷300 μ m):** CPCs mostly adhered to smaller microspheres, covering entirely their surface. Cells also surrounded the edge of larger microspheres. After 24 hours of dynamic culture CPCs were organized in small spherical clusters, suggesting a possible role of the bioreactor in creating a microenvironment suitable for stemness preservation, knowing that sphere formation *in vitro* is a characteristic feature of embryonic and adult SCs (Figure III.19A).

EGFP^{pos} CPCs conjugated to microspheres collected from the bioreactor were then cultured for 5 days in static conditions and subsequently analyzed under inverted and fluorescence microscope. These observations confirmed that CPCs mainly adhered to smaller microspheres. Progenitor cells that were not conjugated to microspheres were also present providing evidence of their viability and proliferative ability. After 5 days of static culture, changes in gelatin/gellan microspheres morphology which suggest the presence of biodegradation were observed (Figure III.19B).

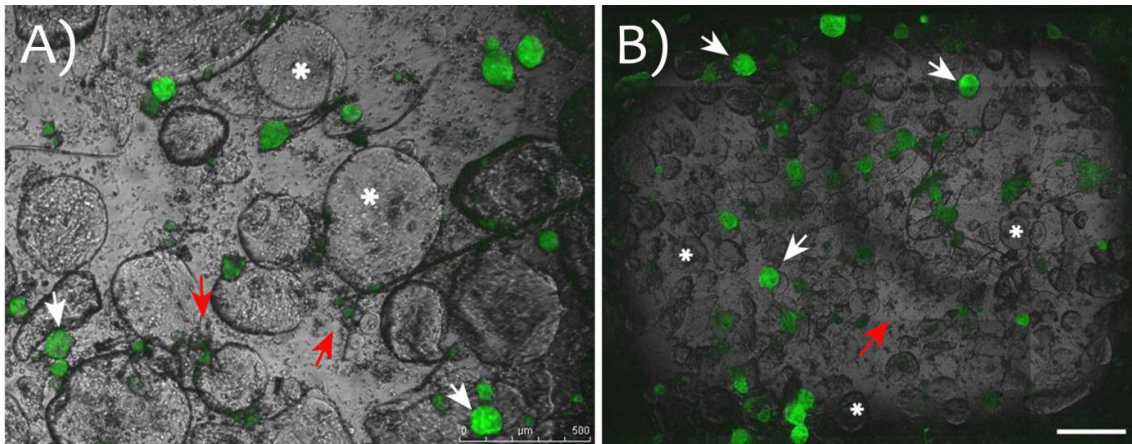


Figure III.19. A) EGFP^{pos} CPCs (green fluorescence) adhered to smaller microspheres (white arrows); microspheres (*) and small clusters of EGFP^{pos} CPCs (red arrows), collected from the culture chamber of the bioreactor after 24h of dynamic culture. Scale bar 500 μm . B) EGFP^{pos} CPCs (green fluorescence) adhered to smaller microspheres (white arrows); microspheres (*) and small clusters of EGFP^{pos} CPCs (red arrows), after 5 days of static culture. Scale bar 1mm.

- **Gelatin/gellan injectable microspheres (diameter 350÷450 μm):** after 24 hours of dynamic culture, CPCs still adhered to microspheres spreading their cytoplasm on microsphere surface (Figure III.20).

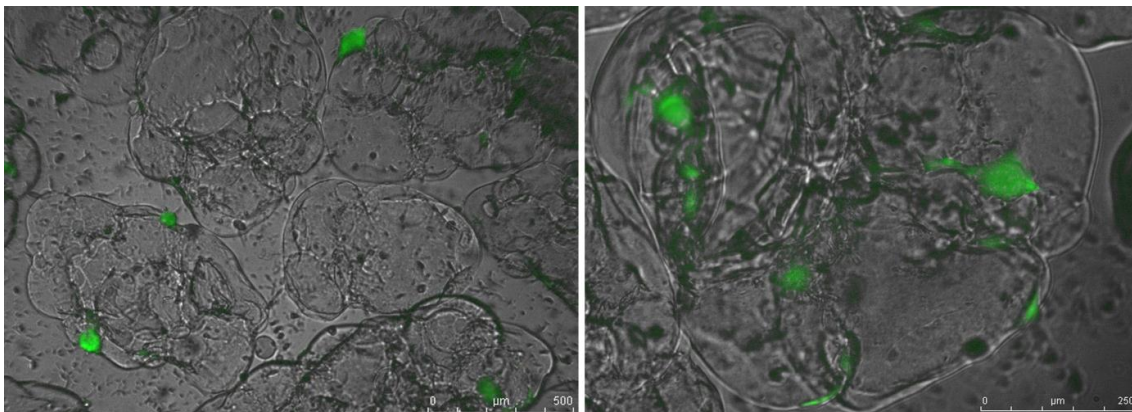


Figure III.20. EGFP^{pos} CPCs seeded on 350 ÷450 μm microspheres after 24h of dynamic culture. Green fluorescence shows adhering cells to microspheres at two different magnifications. Scale bars: 500 μm (left) and 250 μm (right).

After 5 days of static culture, cell and microsphere suspension were analyzed under inverted and fluorescence microscope. We observed that gelatin/gellan injectable microspheres changed their morphology and structure. CPCs were mainly conjugated to microsphere and only few adhered to the culture dish (Figure III.21).

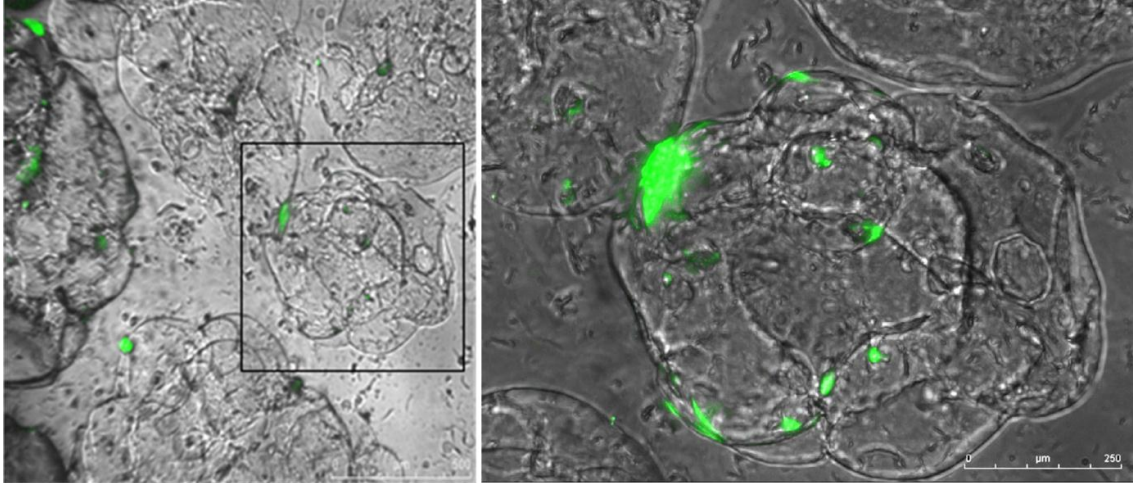


Figure III.21. EGFP^{POS} CPCs seeded on 350 ±450 μm microspheres after 5 days of static culture. Cells adhered to microspheres appear in green fluorescence. Scale bars: 500 μm (left) and 250 μm (right).

- **Gelatin/gellan microspheres functionalized with IGF-1 (d<90 μm):** after 24 hours of dynamic culture, CPCs still adhered to microspheres and at time were laying on microsphere surface. Occasionally, CPCs were found at the interface between two or more microspheres resembling connecting elements (Figure III.22).

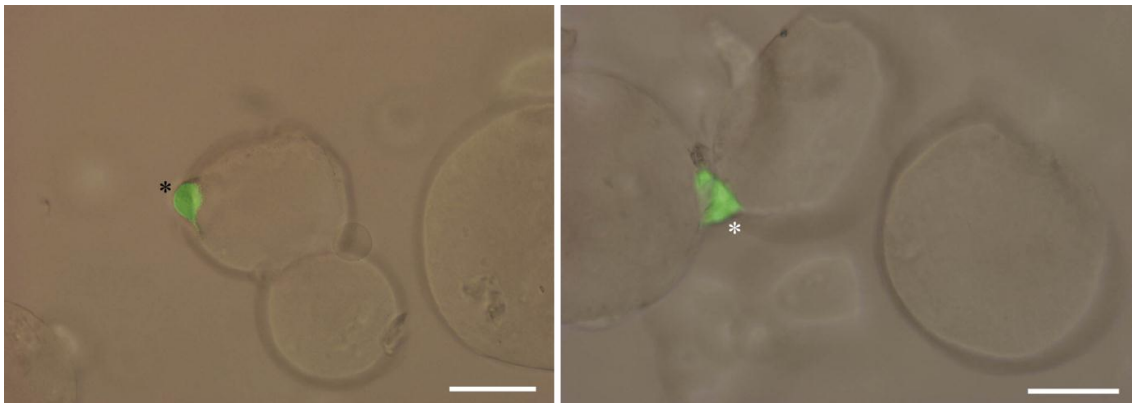


Figure III.22. EGFP^{POS} CPCs (green fluorescence) seeded on microspheres functionalized with IGF-1 d<90 μm after 24h of dynamic culture. Cells adhered to microspheres (black asterisk) or as a connection between two or more microspheres (white asterisk). Scale bars: 50 μm.

After 5 days of static culture, the presence of CPCs still adhering to gelatin/gellan microspheres functionalized with IGF-1 was observed. Cells did not show a round shape and were spreading their cytoplasm over the microsphere surface. Moreover, the presence of both cell-microsphere and cell to cell adhesion was noticed (Figure III.23).

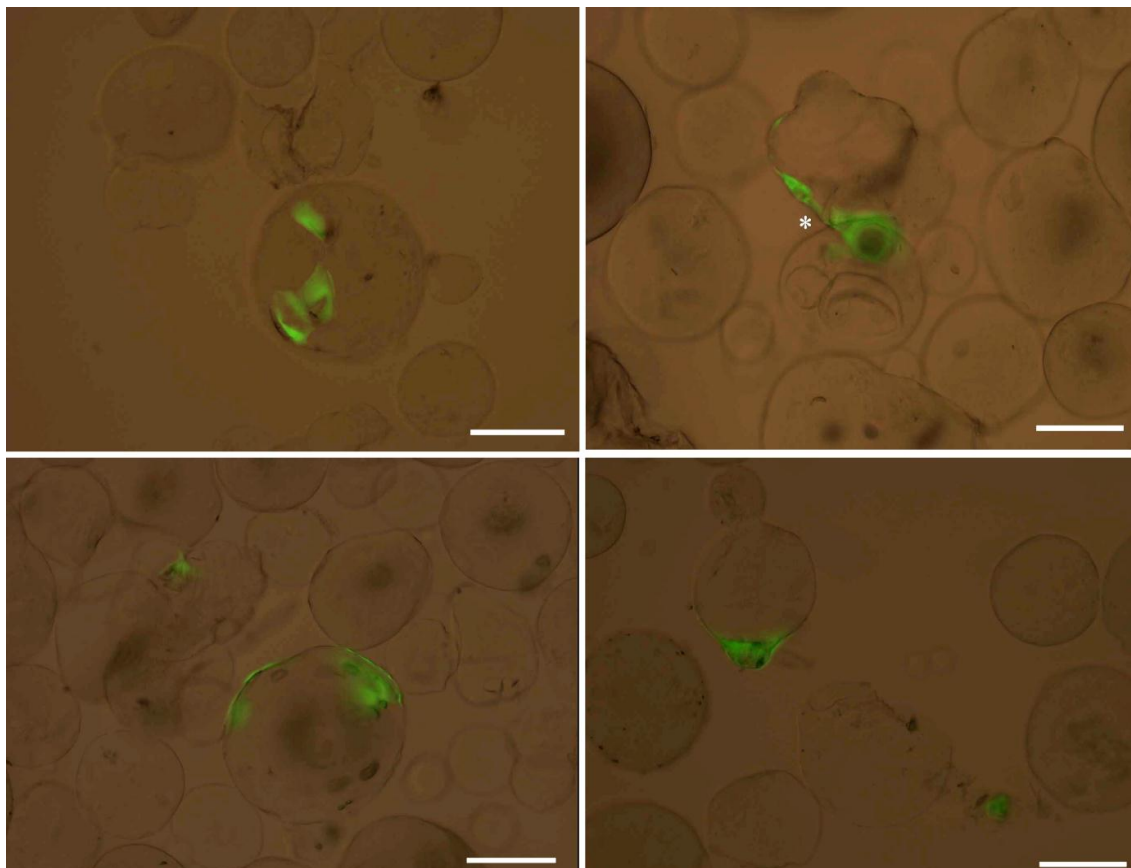


Figure III.23. EGFP^{pos} CPCs (green fluorescence) seeded on microspheres functionalized with IGF-1 $d < 90 \mu\text{m}$ after 5 days of static culture. Cells still adhere to microsphere surface, sometimes connecting cell to cell or cell to microsphere (white asterisk). Scale bars: $100 \mu\text{m}$.

Furthermore, it was observed that virtually CPCs were mainly conjugated with microspheres even if sometimes individual cells were observed to adhere to the dish for as long as 5 days of static culture. This finding suggests a stronger conjugation between single cells and microspheres, likely attributable to IGF-1 functionalization.

Concerning cell-microsphere adhesion, a quantitative assessment of the conjugation of CPCs with microspheres was performed. Obtained results pointed out that after 24 hours of dynamic culture and after 5 days of static culture, a more efficient adhesion of CPCs to smaller microsphere was present. Moreover, an increased cell number was documented after 5 days of static culture, suggesting a positive effect of gelatin/gellan microspheres and dynamic culture in cell proliferation and survival (Figure III.24).

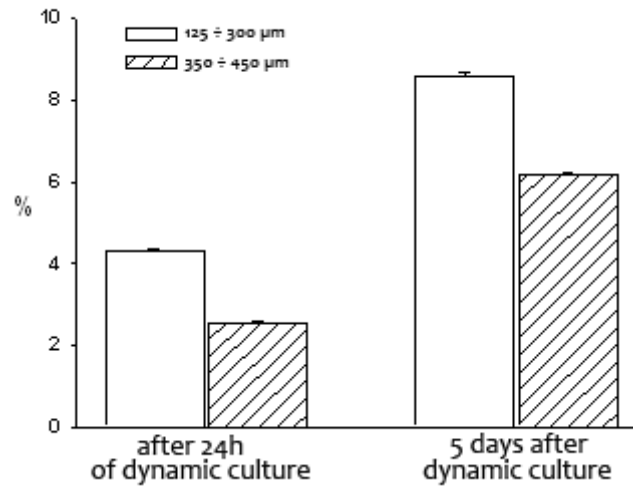


Figure III.24. Quantification of the fractional area occupied by EGFP^{POS} CPCs after 24 hours of dynamic culture and after the following 5 days of static condition.

- **EGFP^{POS} CPCs CTRL:** after 24 hours of dynamic culture, the analysis by inverted microscope showed that EGFP^{POS} CPCs were suspended as single cell; cluster formations were not observed. When seeded, they adhered and grew normally without differences from standard culture condition.

Therefore, findings from preliminary experimental cellular tests established the ability of the bioreactor to guarantee the sterility and the viability of the cell culture, demonstrating the potentiality of this bioreactor that can be used as model system, both for testing cytocompatibility and durability of cell microcarriers (e.g. hydrogel microspheres) and for investigating the influence of suspension condition on cells, with or without microcarriers. In details, results also demonstrated the ability of the bioreactor to establish a biochemical and hydrodynamic environment suitable to maintain the cell-seeded microspheres in suspension condition within an appropriate 3D milieu. Moreover, the formation of small CPC spherical clusters highlights a potential role of the suspension conditions obtained within the bioreactor in creating a microenvironment suitable for stemness preservation.

4. Discussion and Conclusions

Conventional *in vitro* 2D methods, characterized by a static environment with gradient concentrations, strongly differs from the 3D *in vivo* environment, where cells interact each other and with the extracellular matrix in a 3D perfused condition. Depending on the cultured cell types, the 2D unphysiological culture condition can lead to unnatural cell behaviors with altered cell morphology as well. For these reasons, many research groups have looked at developing 3D culture systems in the effort to replicate the 3D biochemical and biophysical native microenvironments.

Suspension culture methods have become the most popular techniques for maintaining specialized features of cells (Hammond and Hammond, 2001), and, with or without microcarriers, they have been adopted for low cost scalable cell expansion and long-term cell viability maintenance (Amit et al., 2010; Zweigerdt et al., 2011; Consolo et al., 2012; Olmer et al., 2012), for guiding differentiation of SCs (Siti-Ismael et al., 2012), for facilitating multicellular aggregate formation (Sen et al., 2001; Cameron et al., 2006; Wang et al., 2006), for preventing the dedifferentiation process that occurs under traditional 2D cell culture conditions (Hammond and Hammond, 2001), and for the production of native-like 3D engineered tissues (Hwang et al., 2009; Yu et al., 2011)

Since current suspension techniques suffer from some limitations, e.g., imposition of non-physiological shear stresses on cultured constructs (roller-bottles, stirred bioreactors), and expensive realization cost (rotating bioreactors), we have developed an innovative multipurpose and low-cost perfusion bioreactor.

Previous studies have widely demonstrated that cells, and especially CMs, need adequate oxygen supply to function efficiently (Carrier et al., 2002; Gerech-Nir et al., 2006; Hecker et al., 2009). Therefore, the possibility to guarantee suitable oxygenation inside a bioreactor is an essential feature that need to be considered in the selection of a bioreactor configuration. Hence, we sized the perfusion subsystem in order to assure a suitable oxygenation of the cell culture, with a consequent proper cell viability, within the bioreactor culture chamber. Two different cases were considered: 1) a fixed number of cells, considering neonatal rat CMs, and 2) a variable number of cells due to proliferation, modeling MSCs. Both studies allowed to find the correct balance among oxygen partial pressure of the medium, cell proliferation and tube length, defining the optimal operating conditions for guaranteeing oxygen level equal to 20%.

Oxygenation is closely linked to the perfusion process within a bioreactor culture chamber. In fact, the beneficial effects of perfusion have been widely demonstrated. In cardiac TE several studies have shown as medium perfusion within suspension culture devices, by enhancing transport of nutrients and waste and providing flow-mediated mechanical stimuli, may benefit the *in vitro* development of 3D tissues and the generation of sufficient amounts of beating CMs for use in cardiac TE (Xu et al., 2006; Niebruegge et

al., 2008; Haraguchi et al., 2013). Moreover, suspension culture with perfusion subsystem integrated generally produced higher cell numbers than static cultures and were able to achieve more aerobic metabolism than static and spinner flask cultures (Teo et al., 2012). The perfusion subsystem has been implemented within our bioreactor for guaranteeing the suspension condition, and also due to its ability to enable a continuous transport of nutrients and supply culture parameters like pH, oxygen, and metabolites maintaining optimal operating conditions throughout the culture period.

Bioreactor configurations that could provide a well-mixed environment have generally shown to improve proliferation of human-derived cell sources like embryonic SCs, (ESCs), MSCs and hematopoietic SCs (HSCs) (Chen et al., 2006; Yirme et al., 2008; Timmins et al., 2012). Differently, hydrodynamics in bioreactors can be optimized to alleviate problems related to static culture in conventional dish, as gradient concentrations and localized extremes that make large-scale bioprocesses difficult to monitor and control. Different bioreactor configurations will result in different flow patterns that can affect cellular activities. For example, hydrodynamics determines the macroscopic environmental conditions that will affect the shear stress and solute transport to the cells.

Shear stresses introduced by the interaction of cells with fluid molecules and bioreactor walls could strongly influence the cell culture, since it poses a direct impact on cell viability and proliferation. It is therefore necessary to optimize the shear environment to ensure high proliferation and viability of the cell sources, and avoiding shear stresses higher respect to the detrimental values for the cells. It has been demonstrated, in fact, that shear stress values higher than 2.5 dyn/cm^2 can cause cellular damage and reduce cell expansion for both human ESC and neonatal rat CM cultures (Dvir et al., 2007; Millman et al., 2009; Lecina et al., 2010). Moreover, other studies have demonstrated as suspension systems with insignificant shear environment produced laminar flow profiles, which serve to minimize cellular damage and increase aerobic metabolism, and as a protective conditioning against apoptosis (Poelmann and Gittenberger-de Groot, 2005; Teo et al., 2012).

In order to investigate the hydrodynamics developing within the culture chamber, CFD simulations could provide a fundamental support. The high efficiency in computational methods enables rapid interrogation of multiple parameters such as mass transfer efficacy, oxygen distribution and shear stress in various bioreactor platforms. Findings from CFD simulations can provide relevant flow information to identify sensitive parameters that are significant to the hydrodynamics of the bioreactor, but can also serve to guide the design of a bioreactor for optimal cell culture (Teo et al., 2012). Accordingly, we performed CFD simulations for assisting the bioreactor design, for studying the microspheres-medium interaction, and for identifying the operating conditions that optimize mass transport e minimize shear stress. In this study the simulations do not take into account the presence of a cellular phase. However, the *in silico* set up could be upgraded in the future by

considering a cellular phase seeded on the suspended microspheres, and by evaluating cell oxygen consumption, as previously proposed (Consolo et al., 2012). Results concerning the shear stress distributions within the culture chamber, lower than $0,17 \text{ dyn/cm}^2$, confirm the suitability of the device to avoid shear stress values critical for cultured cells. Results from preliminary cellular tests demonstrated the ability of the device to guarantee the sterility and the viability of the cell culture. Moreover, after 24 hours of dynamic culture CPCs were found organized in small spherical clusters, suggesting a possible role of the suspension conditions obtained within the bioreactor in creating a microenvironment suitable for stemness preservation, knowing that sphere formation *in vitro* is a characteristic feature of ESCs and adult SCs (Howson et al., 2005; Cormier et al., 2006; Gilbertson et al., 2006; zur Nieden et al., 2007; Ungrin et al., 2008; Kinney et al., 2011). Further cell culture experiments for testing the *in vitro* long-term viability maintenance and sterility, and for investigating the potentiality of the bioreactor as expansion/aggregation/differentiation system of tumorigenic cells (CALU-3, TEpC) and cardiospheres are ongoing and have demonstrated the ability of the bioreactor in maintain the cell culture viability and sterility up to 10 days. The findings of this study clearly demonstrated the suitability of the proposed innovative bioreactor. Thanks to its peculiar geometric features, the device assures the generation of buoyant vortices and the consequent establishment of suspension and low-shear conditions within the culture chamber, without using electromechanical systems. This innovative solution allows to provide a suitable biochemical and hydrodynamic environment for maintaining specimens of different dimensions in suspension conditions, guaranteeing suitable oxygen and nutrient mixing and transport, and avoiding shear stress values affecting the cells. The possibility to obtain suspension conditions with low-shear stress values just using different pressure gradients within the bioreactor, makes this device a low-cost and easy-to-use technological solution compared to the current available techniques.

However, since our bioreactor still suffer from some limitations, future optimizations are now under consideration. First of all, the ability to incorporate *in-situ* monitoring of culture parameters is an essential component in bioreactor design. At the current stage, many real-time monitoring methods are available for bioreactors, including conventional electrochemical sensors, and non-invasive spectroscopic and optical technologies (Beutel and Henkel, 2011; Teixeira et al., 2011). Integration of real-time monitoring technologies should minimize the amount of sample extracted for analysis and any disruption to the cell culture itself. Alternatively *in-situ* probes may be incorporated into the bioreactor and this is one of the most favored designs. However, *in-situ* methods face the challenges of maintaining component sterility and its incorporation into the sterile environment of the bioreactor. The design of a minimally invasive yet reliable monitoring technique remains as one of the main challenges in TE (Teo et al., 2012). Within this scenario we are now investigating the possibility to implement specific sensors and control system

for the on-line, high throughput monitoring of basic parameters such as temperature, pH, partial pressure of oxygen (pO_2) and of carbon dioxide (pCO_2). These functioning modalities will be suitable for a lot of experiments aimed at investigated the environment within the culture chamber, providing the user with several quantitative data to be used to implement a control system of the experimental parameters. Finally, in the next future, in order to 1) reduce the quantity of cell culture medium for minimizing the experimental costs and the number of the bioreactor components for simplifying the use of the system by non-experienced staff, and 2) insert an access side port for allowing cell samples/injections without interrupting the test, modifications of the bioreactor design will be considered.

In conclusion, the innovative bioreactor developed has demonstrated the potentiality to be used as model system, both for testing cytocompatibility and durability of cell microcarriers (e.g. hydrogel microspheres) and for investigating the influence of suspension condition on cells, with or without microcarriers. Preliminary findings suggest that in the next future this bioreactor could be also used as an expansion, aggregation and differentiation system for *in vitro* cell culture.

Acknowledgements

Funding for this study was provided by FP7 European Project BIOSCENT. Gelatin/gellan microspheres were provided by the group of Prof. Giusti (Department of Chemical Engineering, Industrial Chemistry and Materials Science, University of Pisa, Italy). Thermoreversible polyurethane microspheres were provided by the group of Prof. Ciobanu (Petru Poni Institute of Macromolecular Chemistry, Romania). The authors would also like to thank Prof. Quaini (Department of Internal Medicine and Biomedical Sciences, Section of Internal Medicine, University of Parma, Italy) for performing cellular tests.

APPENDIX III.A

Sizing of the perfusion subsystem – Materials and Methods

One of the critical aspects to take into account during bioreactor design is to ensure the adequate oxygenation of the cultured constructs. Therefore, trying to avoid problems related to poor oxygenation, such as cell death or the uneven growth of the tissue, it is fundamental to size the perfusion circuit of the designed bioreactor.

The study, performed in accordance with Orr et al. (Orr et al., 2008), started from a simplified perfusion system (Figure III.A1), where is possible to identify three regions where oxygen exchange takes place.

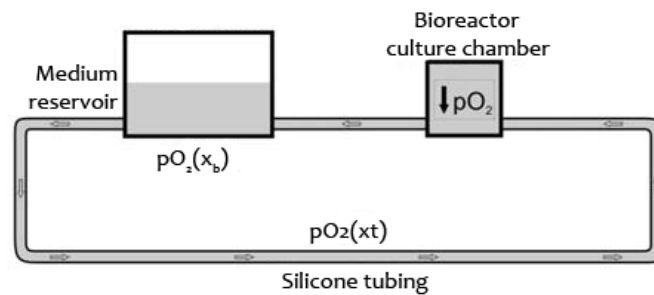


Figure III.A1. Simplified bioreactor system flow circuit. $pO_2(x_t)$ is the partial pressure of oxygen dissolved in the medium at a given length x_t . pO_2 is the partial pressure of oxygen dissolved in the culture chamber. $pO_2(x_b)$ is the partial pressure of oxygen dissolved in the reservoir.

The first region is the culture chamber of the bioreactor, where medium gives oxygen to the constructs and receives carbon dioxide produced by cellular metabolism. The second region is represented by the oxygen-permeable tubes, that allow the oxygen exchange between the contained culture medium and the incubator atmosphere through their wall. Finally, the third region is identified by the free-surface medium reservoir. This latter gives a very low contribution to the oxygen exchange, therefore it was decided to neglect it.

According to Orr et al. (Orr et al., 2008), the content of oxygen gas within the incubator atmosphere was considered to be constant over the duration of any given cell study. On the other hand, oxygen dissolved within the culture chamber decreased due to the cell consumption, while oxygen dissolved in the medium increased over length Δx representing fluid flow through the medium reservoir and silicone tubing, assuming a trend similar to the one shown in Figure III.A2.

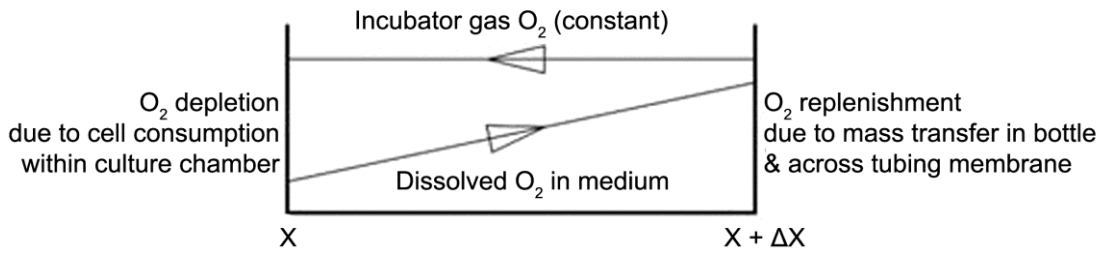


Figure III.A2. Trend of the partial pressure of oxygen (PO_2) along the entire length of the oxygen-permeable tubes.

A Shell Balance has been constructed for the silicone tubing to define the oxygen-permeable tubes' length, in order to obtain an oxygenation equal to the 98% of the oxygen saturation value dissolved within the medium. Assuming a steady-state situation (accumulation = 0), the balanced system for the silicone tubing was examined first using principles from Fournier and Basmadjian.

$$\text{Rate of } O_2 \text{ IN} - \text{Rate of } O_2 \text{ OUT} = 0 \quad (1)$$

$$\left(\frac{Q}{H} pO_2(x) + N_{Avg} \right) - \left(\frac{Q}{H} pO_2(x + \Delta x) \right) = 0 \quad (2)$$

where $C_{O_2} = pO_2 / H$ as determined by the Henry's law, Q is the flow rate delivered by the pump, and H is the oxygen solubility within the culture medium at 37°C .

It has been verified the laminar flow regime inside the tubes for a mean flow rate equal to 400 ml/min ($Re_{\text{mean}} = 1337$). In laminar flow conditions the velocity profile of the medium inside the tubes appears to be parabolic, and for the oxygen mass transport it is reasonable to apply the theory of the two films (Figure III.A3).

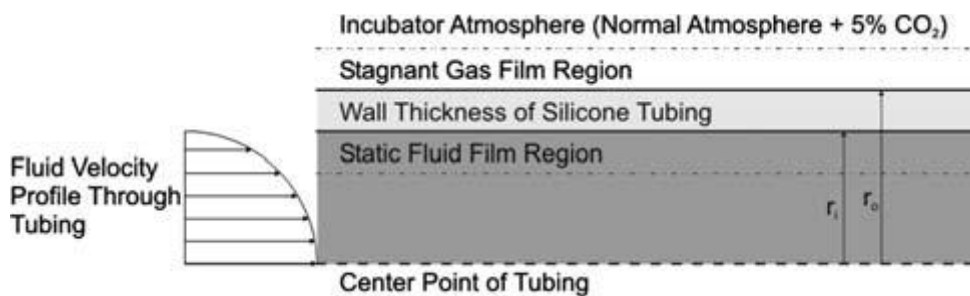


Figure III.A3. Oxygen transport physical model through the wall of the silicone tube.

Near the tube wall a zone of stagnant fluid can be considered (liquid film side). The same condition is present in the incubator side (gas side). Considering as control volume the portion between the two films (gas and liquid film side) and the membrane wall, assuming

the absence of oxygen accumulation inside the volume, the oxygen flow (N_{Avg}) that crosses the side gas is equal to the one that crosses both the liquid film side and the tube wall.

Therefore, N_{Avg} can be expressed with equation 3. The gaseous exchange through the permeable tubes is driven by the partial pressure difference between the incubator side (gas) and the medium side (liquid). Assuming a constant concentration on each cross section of the tube (1D approximation model), the oxygen flow at each section positioned at the coordinate x_t is expressed by the relation

$$N_{Avg} = K_{OL}W\Delta x_t(pO_2' - pO_2(x_t)) \quad (3)$$

where the area of the tubing wall is defined by the product of the log mean of the inner and outer tubing circumference, W , and the change in the tubing length, Δx_t . K_{OL} is the overall mass transfer coefficient. Its inverse (the resistance to the mass transfer coefficient) takes into account the resistance to transport liquid side, solid side, and of the tube wall (function of its permeability):

$$\frac{1}{K_{OL}} = \frac{H}{K_i} + \frac{tmW_i}{\rho_{STP}P_mW} + \frac{RTW_i}{K_oW_o} \quad (4)$$

where:

- W_i , W_o are the inner and outer tubing circumference, respectively;
- ρ_{STP} is the gas density at 0° C and 1 atm;
- R is the gas constant;
- T is the incubator temperature;
- P_m is the silicone tubing oxygen permeability, which is normalized by the wall thickness;
- tm is the thickness of the tube;
- K_i is the mass transfer coefficient of the inner layer;
- K_o is the mass transfer coefficient of the outer layer.

The three summations in the equation 4 can be individually associated with the three layers reported in Figure III.A3. In fact, the model uses three layers representing the ideal barriers through which mass is exchanged between the atmosphere of the incubator and the medium inside the tubes. In detail, the middle layer is the tube wall and is associated with the central term of the equation 4.

$$\left(\frac{tmW_i}{\rho_{STP}P_mW} \right) \quad (5)$$

This term represents the oxygen permeability of the tube wall, which is closely related to the thickness of the tube and its coefficient of permeability.

The first term of equation 4 is associated with the tube inner layer and represents the region of stationary fluid near the wall:

$$\frac{H}{K_i} \quad (6)$$

This region is generated by friction between the stationary fluid in laminar flow and inner wall of the tube.

In order to determine the K_i (liquid film side) coefficient it is necessary to calculate the Reynolds number:

$$Re = \frac{\rho V d_i}{\mu} \quad (7)$$

The density ρ and viscosity μ are assumed equal to 1 g/cm³ and 0.01 g/cm*sec, respectively, and the term V is the mean velocity of fluid in the tube section; if $Re < 2100$ the flow can be considered laminar, and stagnant layer of fluid near the wall is present. The coefficient K_i is then calculated taking into account the correlation existing between Sherwood, Schmidt and Reynolds dimensionless numbers. The Sherwood number is calculated from the following correlation:

$$Sh = 0.43 + 0.53Re^{0.5}Sc^{0.31} \quad (8)$$

where Sc is the Schmidt number expressed as:

$$Sc = \frac{\mu}{\rho D_m} \quad (9)$$

and D_m is the oxygen medium diffusion coefficient at 37°C.

The Shell Balance in equation 1 can be reformulated by combining it with the equation 3:

$$\frac{dpO_2}{dx} = - \frac{K_{OL}WH (pO_2' - pO_2(x_t))}{Q} \quad (10)$$

by integration is obtained

$$pO_2(x_t) = pO_2' - (pO_2' - pO_{2o})e^{\frac{K_{OL}WH}{Q}x_t} \quad (11)$$

In this equation, $pO_2(x_t)$ is the partial pressure of oxygen dissolved in the medium at a given length x_t , pO_2' is the partial pressure of oxygen in the gaseous phase (incubator), and pO_{2o} is the level of oxygen in the medium at the entrance of the tube (that coincides with the partial pressure of oxygen at the exit of the culture chamber).

To determine the pO_{2o} value is necessary to impose a new Shell Balance within the volume of the culture chamber. A cellular component composed by neonatal rat CMs was considered, and the oxygen metabolic consumption value was obtained from literature (Chlopčíková et al., 2001). The partial pressure pO_{2o} can be expressed as

$$pO_{2o} = pO_2(x_t) - \frac{N_{cell}\gamma_{cell}H}{V_{chamber}Q} \quad (12)$$

where N_{cell} is the cell number injected, γ_{cell} is the oxygen metabolic consumption rate for neonatal rat CMs (Chlopčíková et al., 2001), and $V_{chamber}$ is the volume of medium within the culture chamber.

Combining equation 11 and 12 is possible to determine the length of the tube necessary for guaranteeing the proper culture medium oxygenation ($pO_2(x_t)$), following the oxygen metabolic consumption caused by the cellular component within the culture chamber.

$$x_t = - \frac{Q}{K_{OL}WH} \ln \frac{pO_2' - pO_2(x_t)}{pO_2' - pO_{2o}} \quad (13)$$

In Table III.A1 and Table III.A2 the model parameters and the flow rate values with the corresponding Sherwood medium number, mass transfer coefficient K_i , overall mass transfer coefficient K_{OL} , and resistance to the mass transfer coefficient $1/K_{OL}$ are summarized:

Table III.A1. Fluid dynamic and consumption model parameters.

Fluid dynamic parameters		Consumption model parameters	
H (mmHg/ μ M)	0.74	N_{cell}	6×10^5
pO_2' (mmHg)	141	γ_{cell} (mol/cell s)	5.44×10^{-7}
$pO_2(x_t)$ (mmHg)	138.18	V_{chamber} (cm ³)	50
T_m (cm)	0.159		
W_i (cm)	1.995		
W_o (cm)	2.991		
W (cm)	2.459		
ρ_{STD} (mol/cm ³)	4.46×10^{-5}		
R (mmHg/(mM K))	6.24×10^{-2}		
T (K)	310		
P_m (cm ² /mmHg s)	7.96×10^{-8}		
d_i (cm)	0.635		
d_o (cm)	0.952		
ρ (g/cm ³)	1		
μ (g/cm s)	0.01		
$D_{O_2/\text{aria}}$ (cm ² /s)	0.21		
$D_{O_2/\text{medium}}$ (cm ² /s)	2.18×10^{-5}		
Sh_{aria}	0.43		
K_o (cm/s)	0.094		

Table III.A2. Flow rate values with the corresponding Sherwood medium number, mass transfer coefficient K_i , overall mass transfer coefficient K_{OL} , and resistance to the mass transfer coefficient $1/K_{OL}$.

Q (ml/min)	Sh_{medium}	K_i (cm/s)	K_{OL} (mM cm/mmHg s)	$1/K_{OL}$ (mmHg s/mM cm)
400	149,54	$3,42 \cdot 10^{-3}$	$3,96 \cdot 10^{-6}$	$2,52 \cdot 10^5$
300	129,57	$2,97 \cdot 10^{-3}$	$3,50 \cdot 10^{-6}$	$2,86 \cdot 10^5$
200	105,87	$2,42 \cdot 10^{-3}$	$2,93 \cdot 10^{-6}$	$3,42 \cdot 10^5$
100	74,99	$1,72 \cdot 10^{-3}$	$2,14 \cdot 10^{-6}$	$4,67 \cdot 10^5$
90	71,16	$1,63 \cdot 10^{-3}$	$2,04 \cdot 10^{-6}$	$4,90 \cdot 10^5$
80	67,12	$1,54 \cdot 10^{-3}$	$1,93 \cdot 10^{-6}$	$5,18 \cdot 10^5$
70	62,81	$1,44 \cdot 10^{-3}$	$1,82 \cdot 10^{-6}$	$5,51 \cdot 10^5$
60	58,18	$1,33 \cdot 10^{-3}$	$1,69 \cdot 10^{-6}$	$5,92 \cdot 10^5$
50	53,15	$1,22 \cdot 10^{-3}$	$1,55 \cdot 10^{-6}$	$6,44 \cdot 10^5$
40	47,58	$1,09 \cdot 10^{-3}$	$1,40 \cdot 10^{-6}$	$7,15 \cdot 10^5$
30	41,27	$9,45 \cdot 10^{-4}$	$1,22 \cdot 10^{-6}$	$8,19 \cdot 10^5$
20	33,77	$7,73 \cdot 10^{-4}$	$1,01 \cdot 10^{-6}$	$9,93 \cdot 10^5$
10	24,01	$5,50 \cdot 10^{-4}$	$7,23 \cdot 10^{-7}$	$1,38 \cdot 10^6$

Sizing of the perfusion subsystem - Results

In order to guarantee a good cell viability by ensuring an adequate supply of oxygen and nutrient within the culture chamber, the perfusion subsystem was sized. Two different cases have been analyzed: the first one without take into consideration cell proliferation,

whereas the second one considering the cell proliferation in order to take into account the effective experimental test condition.

For the first case, equation 13, the parameters summarized in Tables III.A1 and III.A2, and a partial pressure of oxygen (pO_{20}) at the end of the tubes equal to the 98% of the saturation (138,18 mmHg) were considered. The oxygen exchange due to the free-surface reservoir equal to 0,22 mmHg was neglected.

Table III.A3 reported the lengths of the tubes obtained for each flow rate considered.

Table III.A3. Tube lengths for each flow rate considered.

Q (ml/min)	pO_{20}	Tube length (cm)
400	138,18	0,1
300	138,18	0,2
200	138,18	0,2
100	138,18	0,3
90	138,18	0,3
80	138,18	0,3
70	138,18	0,3
60	138,18	0,3
50	138,18	0,4
40	138,18	0,4
30	138,18	0,5
20	138,18	0,6
10	138,18	3,4

Considering the second case, it is possible to assume that, if a suitable environment establishes within the culture chamber of the bioreactor, during cell culture cells proliferate over time, increasing in number. Therefore, the cell metabolic volumetric oxygen consumption rate will increase and should be considered in the calculation of the necessary tube length for assuring the correct oxygen supply for cell viability. Figure III.A4 shows an overview of the process and the variables involved.

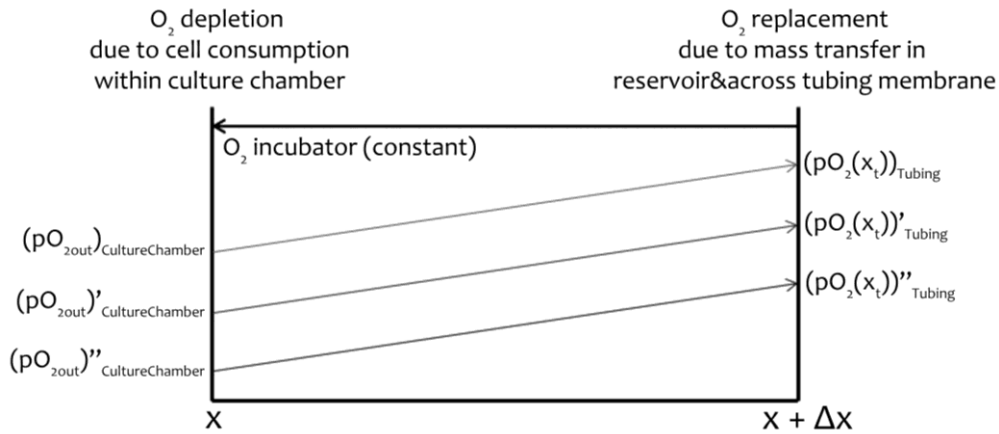


Figure III.A4. Assumption of oxygen replacement in case of cell proliferation; the grey lines represent three different cycles of the culture medium in the bioreactor. The black line represents the constant partial pressure of oxygen within the incubator.

The graph represented in Figure III.A4 shows as, after a series of cycles of the cell culture medium within the perfusion subsystem, there is the possibility that the oxygen consumption is higher than that which can be guaranteed maintaining fixed the length of the tubes. In the graph, the grey lines characterize three different cycles of the culture medium within the bioreactor, representing the variation of the partial pressure of oxygen within the tube at increased instants of time. On the other hand, the black line represents the partial pressure of oxygen within the incubator, which is maintained constant for all the experimental test.

Observing this graph, is possible to determine whether the oxygenation conditions are always maintained at acceptable levels within the culture chamber, guaranteeing suitable cell culture conditions. Contrarily, taking into account the cell proliferation, there is the possibility that the length of the tubes doesn't ensure the suitable oxygenation, bringing the system in hypoxia condition, that occurs for values of partial pressure of oxygen lower than 60 mmHg. Therefore, in order to understand the trend of the partial pressure of oxygen within the culture chamber for a long-term experiment, study was performed. The following equation allows to estimate the cell proliferation trend, modeling MSCs:

$$C_x(t) = C_x(0)e^{\mu t} \quad (14)$$

Where $C_x(0)$ and $C_x(t)$ represent the cell number at the start and at the end of the exponential growth phase, respectively, μ represents the specific growth rate (h^{-1}) and t indicates the time (h) of culture. The value of the growth rate (μ) was assumed equal to $0,22 h^{-1}$ according to the work of Schop (Schop, 2010). Assuming to calculate the proliferation each 1, 4, 8, 16, 24, 36, and 48 hours, and having an initial number of cells equal to 6×10^5 , the following proliferation trend is obtained (Figure III.A5).

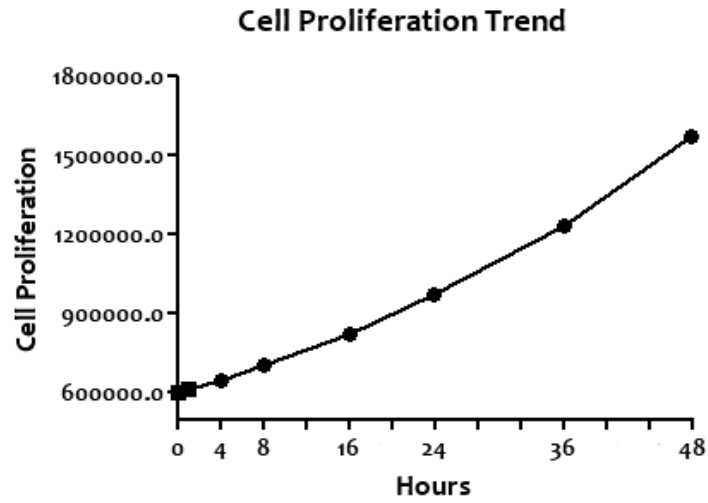


Figure III.A5. Cell proliferation trend.

This proliferation trend is based on the assumption that at each step the cells proliferate similarly, without considering the achievement of the confluence. These data were used to calculate the oxygen consumption at different time step, and the respective length of the tubes necessary to re-establish the optimal oxygenation. In Table III.A4 the tube lengths for each cell proliferation step are summarized.

Table III.A4. Tube lengths for each flow rate and number of cells considered.

Tube length (cm)	Number of cells								
	$6 \cdot 10^5$	$6,12 \cdot 10^5$	$6,50 \cdot 10^5$	$7,04 \cdot 10^5$	$8,26 \cdot 10^5$	$9,70 \cdot 10^5$	$1,23 \cdot 10^6$	$1,57 \cdot 10^6$	
Flow rate (ml/min)	400	0,1	0,1	0,2	0,2	0,2	0,2	0,3	0,4
	300	0,2	0,2	0,2	0,2	0,2	0,3	0,3	0,4
	200	0,2	0,2	0,2	0,2	0,3	0,3	0,4	0,5
	100	0,3	0,3	0,3	0,3	0,4	0,4	0,6	0,7
	90	0,3	0,3	0,3	0,3	0,4	0,5	0,6	0,7
	80	0,3	0,3	0,3	0,4	0,4	0,5	0,6	0,8
	70	0,3	0,3	0,3	0,4	0,4	0,5	0,7	0,8
	60	0,3	0,3	0,4	0,4	0,5	0,6	0,7	0,9
	50	0,4	0,4	0,4	0,4	0,5	0,6	0,8	1
	40	0,4	0,4	0,4	0,5	0,6	0,7	0,8	1,1
	30	0,5	0,5	0,5	0,6	0,7	0,8	1	1,2
	20	0,6	0,6	0,6	0,7	0,8	0,9	1,2	1,5
10	3,4	3,5	3,7	4	4,7	5,5	7	8,9	

Data obtained allow us to conclude that with our tube lengths we are always in safe conditions, guaranteeing the proper oxygenation to the cultured proliferating cells.

References

Amit M, Chebath J, Margulets V, Laevsky I, Miropolsky Y, Shariki K, Peri M, Blais I, Slutsky G, Revel M, Itskovitz-Eldor J. Suspension culture of undifferentiated human embryonic and induced pluripotent stem cells. *Stem Cell Reviews*, 2010, 6(2):248-59.

Andrade-Zaldívar H, Kalixto-Sánchez MA, de la Rosa AP, De León-Rodríguez A. Expansion of human hematopoietic cells from umbilical cord blood using roller bottles in CO₂ and CO₂-free atmosphere. *Stem Cells Development*, 2011, 20(4):593-8.

Beltrami AP, Barlucchi L, Torella D, Baker M, Limana F, Chimenti S, Kasahara H, Rota M, Musso E, Urbanek K, Leri A, Kajstura J, Nadal-Ginard B, Anversa P. Adult cardiac stem cells are multipotent and support myocardial regeneration. *Cell*, 2003, 114(6):763-76.

Beutel S, Henkel S. In situ sensor techniques in modern bioprocess monitoring. *Applied Microbiology and Biotechnology*, 2011, 91(6):1493-505.

Bilodeau K, Mantovani D. Bioreactors for tissue engineering: focus on mechanical constraints. A comparative review. *Tissue Engineering*, 2006, 12(8):2367-83.

Cameron CM, Hu WS, Kaufman DS. Improved development of human embryonic stem cell-derived embryoid bodies by stirred vessel cultivation. *Biotechnology and Bioengineering*, 2006, 94(5):938-48.

Carrier RL, Rupnick M, Langer R, Schoen FJ, Freed LE, Vunjak-Novakovic G. Effects of oxygen on engineered cardiac muscle. *Biotechnology and Bioengineering*, 2002, 78(6):617-25.

Chen X, Xu H, Wan C, McCaigue M, Li G. Bioreactor Expansion of Human Adult Bone Marrow-Derived Mesenchymal Stem Cells. *Stem Cells*, 2006, 24(9):2052-2059.

Chlopcíková S, Psotová J, Miketová P. Neonatal rat cardiomyocytes--a model for the study of morphological, biochemical and electrophysiological characteristics of the heart. *Biomedical papers of the Medical Faculty of the University Palacký, Czech Repub*, 2001, 145(2):49-55.

Choi JS, Kim BS, Kim JD, Choi YC, Lee EK, Park K, Lee HY, Cho YW. In vitro expansion of human adipose-derived stem cells in a spinner culture system using human extracellular matrix powders. *Cell Tissue Research*, 2011, 345(3):415-23.

Consolo F, Bariani C, Mantalaris A, Montevecchi F, Redaelli A, Morbiducci U. Computational modeling for the optimization of a cardiogenic 3D bioprocess of encapsulated embryonic stem cells. *Biomechanics and Modeling in Mechanobiology*, 2012, 11(1-2):261-77.

Cormier JT, zur Nieden NI, Rancourt DE, Kallos MS. Expansion of undifferentiated murine embryonic stem cells as aggregates in suspension culture bioreactors. *Tissue Engineering*, 2006, 12(11):3233-45.

Dvir T, Levy O, Shachar M, Granot Y, Cohen S. Activation of the ERK1/2 cascade via pulsatile interstitial fluid flow promotes cardiac tissue assembly. *Tissue Engineering*, 2007, 13(9):2185-93.

E LL, Zhao YS, Guo XM, Wang CY, Jiang H, Li J, et al. Enrichment of cardiomyocytes derived from mouse embryonic stem cells. *The Journal of Heart and Lung Transplantation*, 2006, 25(6):664-74.

Falvo D'Urso Labate G, Massai D, Pennella F, Gallo D, Montevecchi FM, Morbiducci U, Cerino G. Micro-gravity generating device. Pub. No.: WO/2012/157007, International Application No.: PCT/IT2012/000090.

Fok EY, Zandstra PW. Shear-controlled single-step mouse embryonic stem cell expansion and embryoid body-based differentiation. *Stem Cells*, 2005, 23(9):1333-42.

Freshney RI. *Culture of animal cells*. 2000. Wiley-Liss, New York.

Gerecht-Nir S, Radisic M, Park H, Cannizzaro C, Boublik J, Langer R, Vunjak-Novakovic G. Biophysical regulation during cardiac development and application to tissue engineering. *International Journal of Developmental Biology*, 2006, 50(2-3):233-43.

Gilbertson JA, Sen A, Behie LA, Kallos MS. Scaled-up production of mammalian neural precursor cell aggregates in computer-controlled suspension bioreactors. *Biotechnology and Bioengineering*, 2006, 94(4):783-92.

Goldstein AS, Juarez TM, Helmke CD, Gustin MC, Mikos AG. Effect of convection on osteoblastic cell growth and function in biodegradable polymer foam scaffolds. *Biomaterials*, 2001, 22(11):1279-88.

Goodwin TJ, Prewett TL, Wolf DA, Spaulding GF. Reduced shear stress: a major component in the ability of mammalian tissues to form three-dimensional assemblies in simulated microgravity. *Journal of Cellular Biochemistry*, 1993, 51(3):301-11.

Granet C, Laroche N, Vico L, Alexandre C, Lafage-Proust MH. Rotating-wall vessels, promising bioreactors for osteoblastic cell culture: comparison with other 3D conditions. *Journal of Medical and Biological Engineering*, 1998, 36(4):513-9.

Hammond TG, Hammond JM. Optimized suspension culture: the rotating-wall vessel. *American Journal of physiology. Renal Physiology*, 2001, 281(1):F12-25.

Haraguchi Y, Matsuura K, Shimizu T, Yamato M, Okano T. Simple suspension culture system of human iPS cells maintaining their pluripotency for cardiac cell sheet engineering. *Journal of Tissue Engineering and Regenerative Medicine*, 2013.

Hecker L, Khait L, Radnoti D, Birla R. Novel bench-top perfusion system improves functional performance of bioengineered heart muscle. *Journal of Bioscience and Bioengineering*, 2009, 107(2):183-90.

Howson KM, Aplin AC, Gelati M, Alessandri G, Parati EA, Nicosia RF. The postnatal rat aorta contains pericyte progenitor cells that form spheroidal colonies in suspension culture. *American Journal of Physiology. Cell physiology*, 2005, 289(6):C1396-407.

<http://www.sigmaaldrich.com/labware/labware-products.html?TablePage=9577881>.
Accessed October, 2013.

Hwang YS, Cho J, Tay F, Heng JY, Ho R, Kazarian SG, Williams DR, Boccaccini AR, Polak JM, Mantalaris A. The use of murine embryonic stem cells, alginate encapsulation, and rotary microgravity bioreactor in bone tissue engineering. *Biomaterials*, 2009, 30(4):499-507.

Isu G, Massai D, Cerino G, Gallo D, Bignardi C, Audenino A, Morbiducci U. A novel perfusion bioreactor for 3D cell culture in microgravity conditions. *Proceedings of the ASME 2013 Summer Bioengineering Conference, Sunriver (Oregon-USA) 26-29 June 2013*.

Kehoe DE, Jing D, Lock LT, Tzanakakis ES. Scalable stirred-suspension bioreactor culture of human pluripotent stem cells. *Tissue Engineering Part A*, 2010, 16(2):405-21.

Kinney MA, Sargent CY, McDevitt TC. The multiparametric effects of hydrodynamic environments on stem cell culture. *Tissue Engineering Part B Reviews*, 2011, 17(4):249-62.

Klaus DM. Clinostats and bioreactors. *Gravitation and space biology bulletin*, 2001, 14(2):55-64.

Krawetz R, Taiani JT, Liu S, Meng G, Li X, Kallos MS, Rancourt DE. Large-scale expansion of pluripotent human embryonic stem cells in stirred-suspension bioreactors. *Tissue Engineering Part C Methods*, 2010, 16(4):573-82.

Lecina M, Ting S, Choo A, Reuveny S, Oh S. Scalable platform for human embryonic stem cell differentiation to cardiomyocytes in suspended microcarrier cultures. *Tissue Engineering Part C Methods*, 2010, 16(6):1609-19.

Lee TJ, Bhang SH, La WG, Yang HS, Seong JY, Lee H, Im GI, Lee SH, Kim BS. Spinner-flask culture induces redifferentiation of de-differentiated chondrocytes. *Biotechnology Letters*, 2011, 33(4):829-36.

Liu H, Roy K. Biomimetic three-dimensional cultures significantly increase hematopoietic differentiation efficacy of embryonic stem cells. *Tissue Engineering*, 2005, 11(1-2):319-30.

Marolt D, Augst A, Freed LE, Vepari C, Fajardo R, Patel N, et al. Bone and cartilage tissue constructs grown using human bone marrow stromal cells, silk scaffolds and rotating bioreactors. *Biomaterials*, 2006, 27(36):6138-49.

Millman JR, Tan JH, Colton CK. The effects of low oxygen on self-renewal and differentiation of embryonic stem cells. *Current Opinion Organ Transplantation*, 2009, 14(6):694-700.

Niebruegge S, Nehring A, Bär H, Schroeder M, Zweigerdt R, Lehmann J. Cardiomyocyte production in mass suspension culture: embryonic stem cells as a source for great amounts of functional cardiomyocytes. *Tissue Engineering Part A*, 2008, 14(10):1591-601.

Olmer R, Lange A, Selzer S, Kasper C, Haverich A, Martin U, Zweigerdt R. Suspension culture of human pluripotent stem cells in controlled, stirred bioreactors. *Tissue Engineering Part C Methods*, 2012, 18(10):772-84.

Orr DE, Burg KJ. Design of a modular bioreactor to incorporate both perfusion flow and hydrostatic compression for tissue engineering applications. *Annals of Biomedical Engineering*, 2008, 36(7):1228-41.

Poelmann RE, Gittenberger-de Groot AC. Apoptosis as an instrument in cardiovascular development. *Birth Defects Research. Part C, Embryo Today: reviews*, 2005, 75(4):305-13.

Polatnick J, Bachrach HL. Modifications in the large-scale production of baby hamster kidney cells in roller bottles. *Growth*. 1972 Sep;36(3):247-53.

Qiu QQ, Ducheyne P, Ayyaswamy PS. Fabrication, characterization and evaluation of bioceramic hollow microspheres used as microcarriers for 3-D bone tissue formation in rotating bioreactors. *Biomaterials*, 1999, 20(11):989–1001.

Rodrigues CA, Fernandes TG, Diogo MM, da Silva CL, Cabral JM. Stem cell cultivation in bioreactors. *Biotechnology Advances*, 2011, 29(6):815-29.

Schop D. Cardiac Growth And Metabolism of Mesenchymal Stem Cells Cultivated on Microcarriers. PhD Dissertation, University of Twente, 1982.

Schwarz RP, Wolf DA. (Inventors). Rotating Bio-reactor Cell Culture Apparatus. US patent 4988623. 29 Jan 1991.

Sen A, Kallos M, Behie L. Effects of Hydrodynamics on Cultures of Mammalian Neural Stem Cell Aggregates in Suspension Bioreactors. *Industrial and Engineering Chemical Research*, 2001, 40(23):5350–5357

Siti-Ismail N, Samadikuchaksaraei A, Bishop AE, Polak JM, Mantalaris A. Development of a novel three-dimensional, automatable and integrated bioprocess for the differentiation of embryonic stem cells into pulmonary alveolar cells in a rotating vessel bioreactor system. *Tissue Engineering Part C Methods*, 2012, 18(4):263-72.

Song K, Yang Z, Liu T, Zhi W, Li X, Deng L, et al. Fabrication and detection of tissue engineered bones with bio-derived scaffolds in a rotating bioreactor. *Biotechnology and Applied Biochemistry*, 2006, 45(Pt 2):65–74.

Teixeira AP, Duarte TM, Carrondo MJ, Alves PM. Synchronous fluorescence spectroscopy as a novel tool to enable PAT applications in bioprocesses. *Biotechnology and Bioengineering*, 2011, 108(8):1852-61.

Teo A, Mantalaris A, Lim M. Hydrodynamics and bioprocess considerations in designing bioreactors for cardiac tissue engineering. *Journal of Regenerative Medicine and Tissue Engineering*, 2012, 1(4).

Timmins NE, Kiel M, Günther M, Heazlewood C, Doran MR, Brooke G, Atkinson K. Closed system isolation and scalable expansion of human placental mesenchymal stem cells. *Biotechnology and Bioengineering*, 2012, 109(7):1817-26.

Turhani D, Watzinger E, Weissenbock M, Cvikl B, Thurnher D, Wittwer G, et al. Analysis of cell-seeded 3-dimensional bone constructs manufactured in vitro with hydroxyapatite granules obtained from red algae. *Journal of Oral and Maxillofacial Surgery*, 2005, 63(5):673–81.

Unger DR, Muzzio FJ, Aunins JG, Singhvi R. Computational and experimental investigation of flow and fluid mixing in the roller bottle bioreactor. *Biotechnology and Bioengineering*, 2000, 70(2):117-30.

Ungrin MD, Joshi C, Nica A, Bauwens C, Zandstra PW. Reproducible, ultra high-throughput formation of multicellular organization from single cell suspension-derived human embryonic stem cell aggregates. *PLoS One*, 2008, 13;3(2):e1565.

Wang X, Wei G, Yu W, Zhao Y, Yu X, Ma X. Scalable producing embryoid bodies by rotary cell culture system and constructing engineered cardiac tissue with ES-derived cardiomyocytes in vitro. *Biotechnology Progress*, 2006, 22(3):811-8.

Wolf DA, Schwartz RP. Analysis of gravity-induced particle motion and fluid perfusion flow in the NASA-designed rotating zero-head-space tissue culture vessel. Washington, DC: 1991. (NASA Tech. Paper 3143).

Wolf DA, Schwartz RP. Experimental measurement of the orbital paths of particles sedimenting within a rotating viscous fluid as influenced by gravity. Washington, DC: 1992. (NASA Tech. Paper 3200).

Xu C, Police S, Hassanipour M, Gold JD. Cardiac bodies: a novel culture method for enrichment of cardiomyocytes derived from human embryonic stem cells. *Stem Cells Development*, 2006, 15(5):631-9.

Yirme G, Amit M, Laevsky I, Osenberg S, Itskovitz-Eldor J. Establishing a dynamic process for the formation, propagation, and differentiation of human embryoid bodies. *Stem Cells Development*, 2008, 17(6):1227-41.

Yu B, Yu D, Cao L, Zhao X, Long T, Liu G, Tang T, Zhu Z. Simulated microgravity using a rotary cell culture system promotes chondrogenesis of human adipose-derived mesenchymal

stem cells via the p38 MAPK pathway. *Biochemical and Biophysical Research Communications*, 2011, 22;414(2):412-8.

Yu CB, Lv GL, Pan XP, Chen YS, Cao HC, Zhang YM, Du WB, Yang SG, Li LJ. In vitro large-scale cultivation and evaluation of microencapsulated immortalized human hepatocytes (HepLL) in roller bottles. *The International Journal of Artificial Organs*, 2009, 32(5):272-81.

zur Nieden NI, Cormier JT, Rancourt DE, Kallos MS. Embryonic stem cells remain highly pluripotent following long term expansion as aggregates in suspension bioreactors. *Journal of Biotechnology*, 2007, 129(3):421-32.

Zweigerdt R, Olmer R, Singh H, Haverich A, Martin U. Scalable expansion of human pluripotent stem cells in suspension culture. *Nature Protocols*, 2011, 6(5):689-700.



PART II



CHAPTER IV

Generation of contractile 3D
muscle-like tissue in a perfusion-
based bioreactor culture system

Abstract

Cardiac tissue engineering has shown the potential to generate thick-contractile myocardium-like constructs that might be used as functional substitute or as biological *in vitro* model system to investigate the tissue-specific development and diseases, and to offer accurate and controlled *in vitro* tests for cell and tissue-based therapies, drug screening, predictive toxicology and target validation. The requirements for engineering clinically sized cardiac constructs include the use of biomaterials that might present native-like tissue mechanical properties and/or topographical cues, the application of physiologic conditions such as perfusion, electrical and mechanical stimulation during cell culture, and the choice of a cell population. As a proof-of-principle to engineer thick-relevant skeletal myoblast-based contractile three-dimensional patches we investigated if these requirements can be met by combining cell density, cell culture medium composition, perfusion-based bioreactor culture system parameters, and type I collagen scaffold. We demonstrate that this combined approach resulted in increased viability, and functionality of the cardiac patch. After 6 days of perfused culture within a bioreactor-based culture system, skeletal myoblast-seeded on millimeter-thick cardiac patches displayed significantly improved viability, survival and differentiation of skeletal myoblasts, leading to greatly enhanced contractility. Perfusion also improves the seeding phase, resulting in a more homogeneous distribution of the cells within the entire volume of the scaffold. We propose that these techniques can be utilized to engineer reproducible thick-relevant and compact skeletal myoblast-based contractile three-dimensional patches, for the formation of engineered cardiac tissue to be used as functional substitute or as biological *in vitro* research model system.

Keywords: cardiac tissue engineering, bioreactor, perfusion, differentiation, skeletal myoblasts.

1. Introduction

Cardiac tissue engineering (TE) has shown the potential to generate functional myocardium-like constructs that might be used as functional substitute or as biological *in vitro* model system (Bursac et al., 1999; Habeler et al., 2009; Smits et al., 2009; Hirt et al., 2012), e.g. for drug screening, predictive toxicology and target validation (Elliot and Yuan, 2010; Hansen et al., 2010).

Cardiac TE implies the use of biomaterials that might present native-like tissue mechanical properties and/or topographical cues (Kim et al., 2010), as well as applying physiologic conditions such as perfusion (Radisic et al., 2008), electrical (Tandon et al., 2009) and mechanical stimulation (Fink et al., 2000; Zimmermann et al., 2002a; Gonen-Wadmany et al., 2004; Birla et al., 2007) during cell culture (Chiu and Radisic, 2013, Massai et al., 2013).

The choice of which cell population to employ for cardiac TE should meet some key requirements as the availability in large numbers and the ability to differentiate into cardiac lineages able to survive and function (Vunjak-Novakovic et al., 2010; Chiu and Radisic, 2013). Neonatal rat cardiomyocytes are often chosen for their natural electrophysiological, structural, and contractile properties (Zheng et al., 2012; Ravichandran et al., 2013), however they have a limited capacity to proliferate and not clinical relevance. Embryonic stem cells (ESCs) (Boheler et al., 2002; Mummery et al., 2002; Guo et al., 2006; Zimmermann and Eschenhagen, 2007) and induced pluripotent stem cells (iPSCs) (Mauritz et al., 2008, Narazaki et al., 2008; Martinez-Fernandez et al., 2009; Zwi-Dantsis et al., 2011) represent valid cell candidates for cardiac TE thanks to their autologous nature, ability to propagate in large quantities, and to differentiate into cardiomyocytes. However, their still high risk of tumorigenicity and the complexity of their differentiation protocols still make it not an easy cell source to be used for safe and standardized cardiac TE. Human adult stem cells (Scs) share most of the positive features with iPSCs making them an eligible cell candidate for cardiac TE with the extra benefit of low oncogenesis, but have shown to have still a limited and not highly reproducible *in vitro* differentiation potential into fully mature cardiomyocytes (Orlic et al., 2001; Beltrami et al., 2003; Planat-Benard et al., 2004). Skeletal myoblasts (SMs) are widely used in cardiac TE thanks to their high proliferative potential, high resistance to ischemia, and their fate restriction to the myogenic lineage, with the capacity to develop a complete contractile apparatus, virtually eliminates the risk of tumorigenicity (Manasché, 2004; 2008). On the other hand, the major disadvantage of SMs is that they do not electrically couple with the host cardiomyocytes (Durrani et al., 2010), and this obviously raises the major question of the mechanisms by which, in case of cell transplantation, the myoblasts can improve left ventricular function (Manasché, 2004). Despite this concern, several research groups have demonstrated the ability of SMs to partially treat cardiomyopathies both in small (Khan et al., 2007; Al Attar et al., 2003; Ye at

al., 2005; Taylor et al., 1998; McCue et al., 2008) and large animal models (Ghostine et al., 2002; Haider et al., 2004; Brasselet et al., 2005; He et al., 2005; Hata et al., 2006; Ye et al., 2007). However, cell transplantation often results in tissue damage and poor cell engraftment limiting therefore the potential application of SM-associated therapies (Hamdi et al., 2011). Cardiac TE might overcome this limitation by culturing progenitor cells on biomaterial scaffolds (designed to provide a structural and logistic template for tissue development) in bioreactors (designed to control cellular microenvironment, facilitate mass transport to the cells and provide the necessary biochemical and physical regulatory signals) in order to develop *in vitro* an appropriate cell environment to support both cell survival and differentiation upon implantation (Siepe et al., 2007, Hamdi et al., 2011). Several studies have demonstrated as SMs seeded on polymeric scaffolds, as polyurethane, or biological scaffolds, as collagen type I, implanted on infarcted hearts, were able to migrate from the patch to the damaged myocardium (Siepe et al., 2007; Kroehne et al., 2008; Ma et al., 2011). Improved functions were later observed by statically loading genetically modified SMs on three-dimensional (3D) scaffolds, obtaining an enhanced angiogenesis, and a reduced infarction zone (Blumenthal et al., 2010; von Wattenwyl et al., 2012).

Based on our knowledge, 3D SM-based constructs have been generated only by static condition until now, whereas bioreactor-based culture could offer a high control over the culture parameters and therefore lead to a standardized and reproducible production process. In particular, perfusion-based bioreactor methods for cell seeding and culture result in an increase of cell loading efficiency, and in the formation of functional cardiac engineered tissue with a relevant thickness by promoting homogeneous distribution of oxygen and nutrients, and in enhanced expression of cardiac-specific markers (Carrier et al., 1999; 2002a; 2002b; Radisic et al., 2003). In this study, we therefore aim to investigate the perfusion-based culture parameters suitable to engineer reproducible thick-relevant contractile 3D patches starting with mouse SMs and type I collagen scaffold. In particular, we focused on the influence of initial cell density and of different culture medium composition on the ability of SMs to proliferate and differentiate into contractile units in a 3D bioreactor-based culture system.

2. Materials and Methods

2.1 Cell culture

Primary myoblasts isolated from C57BL/6 mice were transduced with a retrovirus expressing the β -galactosidase (LacZ) marker gene, as previously described (Rando and Blau, 1994), and cultured in 5% CO₂ on collagen-coated dishes, with a growth medium consisting of 40% DMEM low glucose (Sigma-Aldrich Chemie GmbH, Steinheim, Germany), 40% (v/v) F-10 (Sigma-Aldrich Chemie GmbH, Steinheim, Germany), 20% (v/v) FBS (HyClone,

Logan, UT), supplemented with 2.5 ng/ml FGF-2 (R&D Systems, Abingdon, UK), 1% (v/v) P/S, and 1% (v/v) glutamine. When 70% confluence was reached, cells were detached by using 0.25% (w/v) trypsin/0.1% (w/v) EDTA and then used in the experiment.

2.2 Polymer scaffold

In this study a commercially available type I collagen scaffold (Ultrafoam® collagen hemostat from Davol Inc., Cranston, RI), highly porous material, ~ 90% void volume with interconnected pores 100–200 µm in diameter (Radisic et al., 2003; Meinel et al., 2004a; 2004b), was used as discs of 12 mm diameter, 3 mm thickness. Immediately before use, each collagen scaffold was hydrated in culture medium (24 h in the 37°C at 5% CO₂ humidified incubator).

2.3 Perfusion-based bioreactor culture system

For the direct perfusion of a cell suspension through the pores of 3D scaffolds, a previously developed bioreactor was used (Wendt et al., 2003). As shown in Figure IV.1, scaffold was placed between two silicon O-rings which were holding it in place and allow perfusion of the medium through the collagen sponge voids, as shown in Figure IV.1. Therefore, only the inner 8-mm core of collagen scaffolds was directly perfused. The polycarbonate culture chamber that was attached to two silicone columns and connected to a syringe pump (Programmable Harvard Apparatus PHD ULTRA™ 2000)



Figure IV.1. Positioning of the scaffold within the polycarbonate bioreactor culture chamber.

2.4 Cell preparation and scaffold seeding

Engineered constructs were prepared using SMs. Scaffolds were placed into custom produced chambers of the perfusion-based bioreactor culture system, and seeded with a cell density of 2.2×10^6 or 3.3×10^6 cells per scaffold and at a forward-reverse flow rate of 3ml/min for 24 hours, as described in previous studies (Scherberich et al., 2007). The cell-seeded constructs were then cultured with a bidirectional perfusion flow rate of 0.15 ml/min for an additional 5 days. Depending on the experiment, cells were seeded and cultured on the scaffolds in either of the following media: (a) SM proliferation medium

(PM) consisting of 40% DMEM low glucose (Sigma-Aldrich Chemie GmbH, Steinheim, Germany), 40% (v/v) F-10 (Sigma-Aldrich Chemie GmbH, Steinheim, Germany), 20% (v/v) FBS (HyClone, Logan, UT), supplemented with 2.5 ng/ml FGF-2 (R&D Systems, Abingdon, UK), (b) SM differentiation medium (DM) containing 95% DMEM low glucose (Sigma-Aldrich Chemie GmbH, Steinheim, Germany), 5% (v/v) horse serum (Invitrogen, Basel, Switzerland), and (c) a SM complete medium (CM) consisting of 90% DMEM high glucose (Sigma-Aldrich Chemie GmbH, Steinheim, Germany), 10% (v/v) FBS (Sigma-Aldrich Chemie GmbH, Steinheim, Germany). All media were supplemented with 1% (v/v) P/S, and 1% (v/v) glutamine. Cell culture medium was changed every 2/3 days.

Layout of the experimental plan is reported in Figure IV.2.



Figure IV.2. Layout of the experimental plan.

2.5 DNA quantification

One half of each construct was weighed and digested overnight at 57°C in 1 mL of proteinase K solution (1 mg/ml proteinase K, 50 mM TRIS, 1 mM EDTA, 1mM iodoacetamide, and 10 µg/ml pepstatin-A; Sigma-Aldrich, USA) in double distilled water or potassium phosphate buffer. DNA quantification was performed by means of a commercially available fluorescence based kit, namely CyQUANT® Cell Proliferation Assay (Invitrogen, Switzerland). Working solutions were prepared according to the manufacturer's protocols. The analyses were carried out measuring fluorescence with a Spectra Max Gemini XS Microplate Spectrofluorometer (Molecular Devices, USA). Excitation and emission wavelengths were respectively 485 nm and 583 nm. Samples in each plate included a calibration curve. Each sample was measured in triplicate.

2.6 Cell seeding efficiency

The seeding efficiency, defined as the percentage of initially seeded cells that attached to the scaffolds, was determined by comparing the DNA content present in each scaffold after 24 h of perfusion seeding to the reference DNA value determined for aliquots of the seeding cell suspension. For reference samples (corresponding to the total amount of cells loaded per scaffold), cells were centrifuged to obtain pellets, digested in 1 mL of proteinase K solution (1 mg/ml proteinase K, 50 mM TRIS, 1 mM EDTA, 1mM iodoacetamide, and 10 µg/ml pepstatin-A; Sigma-Aldrich, USA), and analyzed using the CyQUANT® Cell Proliferation Assay (Invitrogen, Switzerland). As these samples contained the same number of cells initially seeded per scaffold, they served as a reference (100% value) for seeding efficiency. For cultured constructs, samples were cut in half and weighed, digested in 1 mL of proteinase K solution, and analyzed using the CyQUANT® Cell Proliferation Assay (Invitrogen, Switzerland). Working solutions were prepared according to the manufacturer's protocols. The analyses were carried out measuring fluorescence with a Spectra Max Gemini XS Microplate Spectrofluorometer (Molecular Devices, USA). Excitation and emission wavelengths were respectively 485 nm and 583 nm. The linear relationship of the CyQuant fluorescence with the cell number allowed us to directly calculate the seeding efficiency as the ratio of measured values.

2.7 Immunofluorescence microscopy and quantitative analysis of myotubes

For fluorescence imaging, one half of each cultured scaffold was fixed overnight in 1% paraformaldehyde, and the second day again overnight in 30% sucrose. All the previous steps were performed at 4°C. The third day cultured scaffolds were embedded in OCT (CellPath, Newtown, Powys, UK), sectioned in 10 and 25 µm thick sections through the cross-section of the scaffold by means of a cryostat (Microm International GmbH, Walldorf, Germany). Construct sections were incubated for 1 h in 0.3% Triton X-100 and 2% normal goat serum in PBS (at room temperature), and then for 1 hour (at room temperature) in mouse monoclonal anti-desmin (Mubio Products, Switzerland) primary antibody at 1:100. Subsequently, tissue sections were incubated in dark for 1 h (at room temperature) in Alexa546 anti-mouse (Invitrogen, Switzerland) secondary antibody at 1:200. Nuclei were stained using DAPI (Invitrogen, Switzerland) at 1:50 for 1 h (at room temperature). Antibodies were diluted in 0.3% Triton X-100 and 2% normal goat serum in PBS. Fluorescence images were taken with 20x on an Olympus BX63 Apollo fluorescent microscope (Olympus, Volketswil, Switzerland). All image analyses were performed using ImageJ 1.47 software (Research Service Branch, NIH, USA).

2.8 Calculation of fusion and maturation indices

The fusion index was calculated as the ratio of the nuclei number in desmin-positive myocytes with two or more nuclei versus the total number of nuclei (Bajaj et al., 2011). The maturation index was defined as myotubes having five or more nuclei (Bajaj et al., 2011). The graphs were created in GraphPad Prism 5 (GraphPad Software Inc., USA), and Photoshop CS5 (Adobe Photoshop Software Inc., USA) was used for assembly of figures.

2.9 In vitro contractility assessment

The assessment of the *in vitro* contractility was performed in organ baths (TSE, Bad Homburg) containing 12 ml of KH solution 20x, 4.2g of sodium bicarbonate, 4g of glucose, 1.25 mM CaCl₂, sodium L-ascorbate in deionized water at 37°C equilibrated with Carbogen Gas (95% O₂; 5% CO₂). Cultured scaffolds were punched at 8 mm diameter and attached vertically between a rigid and a mobile fastening (steel hooks) as shown in Figure IV.3.

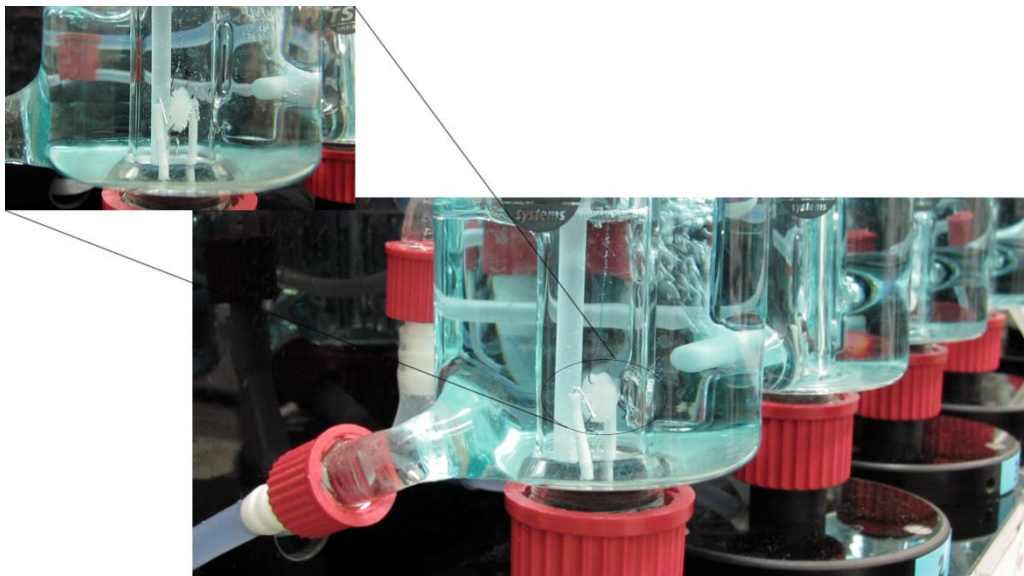


Figure IV.3. Picture of the organ bath set-up.

The latter was connected to a force transducer. The constructs were preloaded with a force of 300 mg and electrically paced with rectangular pulses (10 ms pulse duration, 100 mA pulse amplitude) field stimulation at 1 Hz. The contractility measured by the force transducers was continuously recorded on a PC using BioSys-software (TSE, Bad Homburg) with or without the application of electrical stimulation (ES). Functionality was assessed in duplicates. The amplitude of contraction was then measured as the maximum minus the minimum force recorded in mg.

2.10 Statistical analysis

Data were analyzed using the analysis of variance one-way ANOVA followed by Bonferroni's post-hoc tests for multiple comparison using GraphPad Prism 5 (GraphPad Software Inc., USA). Results were considered statistically significant when the p value was less than ($p < 0.05$). The data are shown as mean \pm standard error on the mean (SEM). The number of replicate experiments performed is given as n.

3. Results

3.1 Evaluation of cell-scaffold interaction

Two different cell densities were investigated to define the suitable initial cell number (assessed by cell seeding efficiency) to support SM differentiation (assessed by immunofluorescence for desmin). When 2.2×10^6 cells were loaded per scaffold, the seeding efficiency was found to be higher than 70%, corresponding to an average of ~ 1.54 millions of adherent cells, but no differentiation in myotubes and neither construct contraction were observed (data not show). However, when 3.3×10^6 cells/scaffold were used, cell seeding efficiency was found to be higher than 55%, corresponding to ~ 1.8 million cells attached to the scaffold and the resulting engineered constructs were capable to contract. These results suggested that there might be an upper limit of cell number which is feasible to be loaded at one time on collagen disc of 8 mm diameter and 3 mm thickness. The cell density of 3.3×10^6 cells/scaffold resulted to maximize seeding efficiency and differentiation process, while minimizing cell waste, and thus this seeding density was used for the subsequent experiments.

In vitro two-dimensional (2D) SM differentiation highly depends on the initial cell density and on the supplementation of serum in the culture medium. In our bioreactor 3D culture system, we investigated the fate of SMs when cultured in 3D with a medium either pushing SM proliferation or SM differentiation or a medium normally used for stem cell or neonatal CM culture for up to 6 days under perfusion. As shown in Figure IV.4, DNA quantification results indicated that the cell number was higher when cultured with PM or CM as compared to DM after 5 days of culture. The cell number presents on the constructs cultured for 5 days with DM corresponded to only the 3.4% of the cells initially adherent to the scaffold.

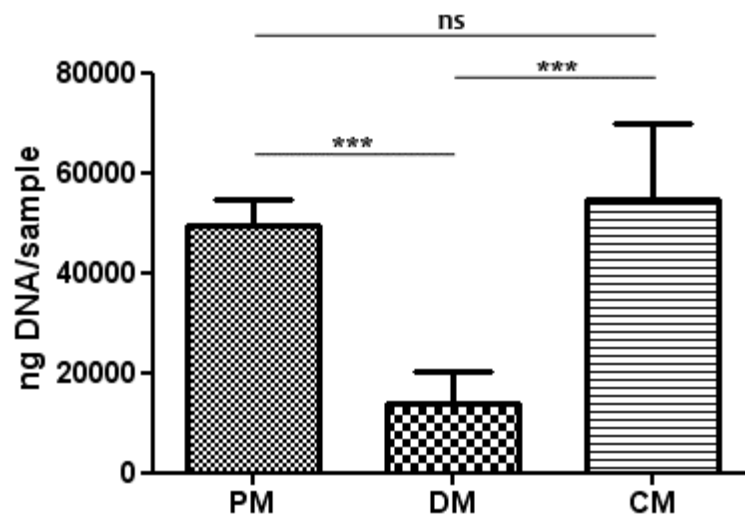


Figure IV.4. Total DNA quantification analyses. Significance: *** $p < 0.001$, and ns = not significant. Data are represented as mean \pm SEM. ($n = 3$).

Taken together, these results demonstrated the feasibility to appropriately seed SMs on the porous collagen substrate and suggest the possibility to regulate their growth fate with the use of exogenous factors during the perfusion culture.

3.2 Fusion and maturation indices of SM

When deprived of serum SMs undergo cell cycle arrest and start to fuse together to form long multinucleated myotubes, useful as contractile unites, and as the building blocks for cardiac muscle. Desmin specific staining was used to assess the initial SM fusion into myotubes. Immunofluorescent staining for desmin and nuclei showed that cells were spatially uniformly distributed throughout the entire volume of the constructs, as expected after the culture in a perfusion-bioreactor system. Cells positive for desmin were also present uniformly throughout the cross section of the generated constructs. However, tissues engineered in CM resulted to have higher amount of desmin-positive cells (Figure IV.5).

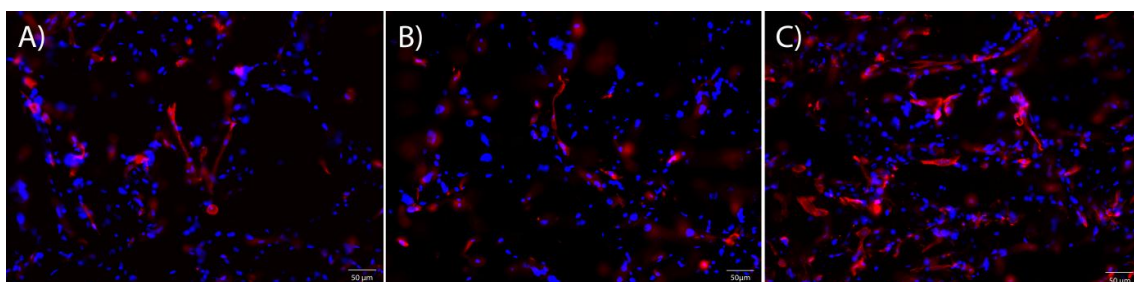


Figure IV.5. SM differentiation. Fluorescent images for desmin of the SM cultured on the collagen scaffolds with different cell culture medium: PM (A) or DM (B) or CM (C). Cells were stained for anti-desmin (red) and DAPI (blue). Scale bar = 50 μ m.

To assess and quantify the differentiation of myotubes, we calculated the fusion index determining the number of nuclei in the desmin stained myotubes (only cells with ≥ 2 nuclei were used) normalized to the total number of nuclei in the field of view. The results reported in Figure IV.6 show a progressive increase in myotube differentiation starting with the PM followed by DM and CM. CM (3.74 ± 0.34) showed greater than 3 and 2-fold differentiation compared to PM (1.24 ± 0.22) and DM (1.87 ± 0.41), respectively. The maturation index (% of myotubes ≥ 5 nuclei) was also used as a parameter to evaluate the differentiation of SMs. The maturation index can also be used to quantify the size of the myotube, a higher maturation index represents myotube larger in size (Sun et al, 2010; Bajaj et al., 2011) (Figure IV.6). Constructs generated in CM resulted to have both the highest fusion and maturation index. The maturation index for the CM (28.26 ± 2.41) was statistically higher than that for the PM (9.44 ± 0.78), and DM (20.65 ± 2.84).

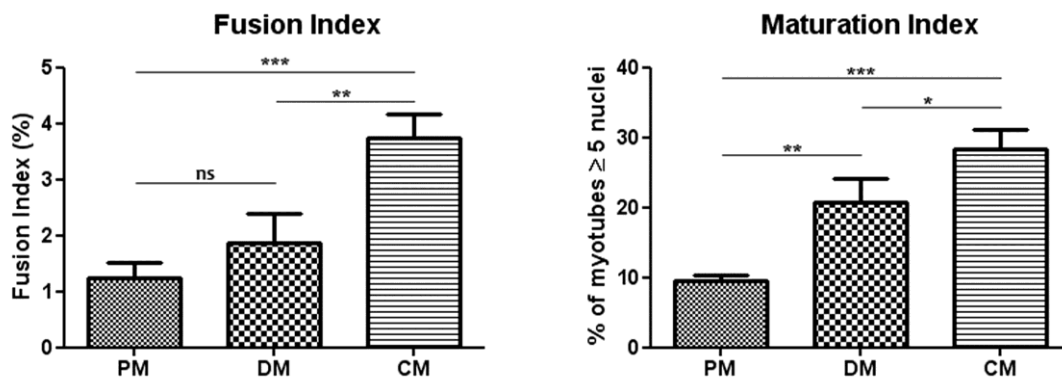


Figure IV.6. Quantification of the fusion and maturation index for the SM cultured with different cell culture medium. (A) Fusion Index. The fusion index was calculated as the ratio of the nuclei number in myocytes with two or more nuclei versus the total number of nuclei. (B) Maturation Index. The maturation index was defined as myotubes having five or more nuclei. Significance: *** $p < 0.001$, ** $p < 0.01$, * $p < 0.05$, and ns = not significant. Data are represented as mean \pm SEM. ($n = 3$).

3.3 In vitro assessment of the contractility

Engineered constructs cultured in CM resulted also to contract better than those generated in PM either with or without the application of ES (Figure IV.7). Engineered tissues generated in DM did not contract spontaneously or after pacing. Those functional results are in agreement with the maturation and fusion index results assessed by image analysis (Figure IV.6).

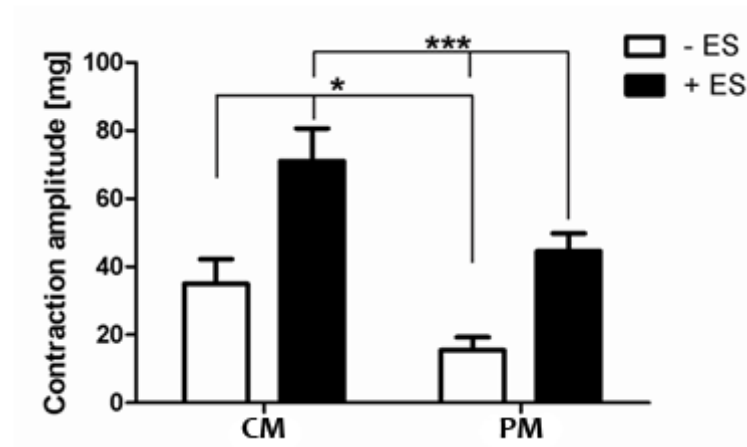


Figure IV.7. Graph representing the amplitude of contraction force (expressed in mg) of SM-based constructs cultured in CM or PM assessed in organ bath with (+ES) or without (-ES) electrical stimulation (+ES corresponds to the stimulation with a pulse of 10 ms duration and 100 mA of amplitude at the frequency of 1 Hz).

Significance: * $p < 0.01$ and *** $p < 0.0001$. Data are represented as mean \pm SEM. (n = 3).

4. Discussion

In this study, we have demonstrate the possibility to engineer thick-relevant SM-based contractile 3D patches to be used as functional substitutes or as biological *in vitro* research model systems in perfusion-based bioreactor. We identify the CM as the most suitable culture condition among those investigated to promote both SM growth and differentiation, leading to a significant functional improvement. It is well known the crucial role of cell culture medium composition in SM differentiation (Goto et al., 1999; Portiér et al., 1999; Lawson and Purslow, 2000; Yoshiko et al., 2002); however, in static culture conditions we do not observe similar effects than in perfusion culture with the same use of medium composition. Perfusion culture and 3D system might have a crucial effect. Notably, the effect induced by the perfusion stimulation was efficient enough to allow survival and differentiation of the SMs inside a millimeter-thick cardiac patch and therefore contractility of the cardiac patches.

Over the past decade, advances in the field of cardiac TE have been achieved through the application of various types of biophysical stimuli: electrical (Radisic et al., 2004), mechanical (Zimmermann et al., 2002b), and hydrodynamic (Carrier et al., 2002b), via specialized bioreactors. Generally, the bioreactor designs have been motivated by the understanding of the native cardiac environment, and the notion that the factors present in the developing cardiac tissue *in vivo* need to be recapitulated to engineer functional cardiac tissues *in vitro*.

Among these biophysical stimuli, the hydrodynamic one obtained through perfusion-bioreactor, by reducing diffusional gradients associated with mass transport over

macroscopic distances and improving control of local levels of pH and oxygen, is essential to maintain the viability and function of cardiac patches. Previous studies demonstrated that perfusion improves cell seeding efficiency throughout the thickness of 3D scaffolds, promotes homogeneous distribution of oxygen within a bioreactor culture chamber, increases construct thickness, enhances the expression of cardiac-specific markers (Carrier et al., 1999; 2002a; 2002b; Radisic et al., 2003), and guarantees high cell viability by protecting cells from critical hydrodynamic shear (Maidhof et al., 2010). In the present study, significant improvements of the differentiation process, and of the contractility on the cardiac patch, critically depended on the use on a perfusion-based bioreactor culture system, as culturing without perfusion could not rescue cardiac contractility.

Initially, focus was given on the cell density. In fact, it has been demonstrated as the seeding step is especially critical to the homogeneity of the construct but also to the efficiency of the production process (Wendt et al., 2003). Within the present experimental setup, the number of cells loaded through the bioreactor system was defined by optimizing the seeding efficiency and yielding a final amount of adherent cell in a range that has been previously reported to prime cell proliferation and extracellular matrix synthesis (Zhou et al., 2006). Moreover, the cell density used was chosen by improving the differentiation process, as with the lower density no signs of fusion were observed.

Concerning seeding, perfusion of a cell suspension through the pores of collagen scaffolds proved to be effective in seeding cells at high densities, an important factor in engineering tissues that mimic the physiologic cell density, and allow to achieve homogeneous spatial distribution throughout the construct volume. We selected a flow rate equal to 3 ml/min for seeding based upon a previous study (Maidhof et al., 2010) that showed perfusion of a cell suspension through highly porous scaffold could be achieved with linear flow rates ranging from 0.6 – 6 ml/min. For culture, medium perfusion at 0.15 ml/min induced efficient assembly of compacted cardiac tissue, suggesting that our selected flow rate was suitable for SM culture.

Another key requirement is to maximize the cell seeding efficiency and to support cell viability achieved by limiting the relatively high flow rate to the initial seeding for only 24 h period. It has been demonstrated, in fact, that the used seeding technique with (i) rapid inoculation of cells into collagen sponges, (ii) immediate establishment of the interstitial flow of culture medium through the seeded scaffolds, and (iii) forward-reverse flow used for the initial period of 24 h in order to further increase the spatial uniformity of cell seeding, is particularly suitable for cardiac TE (Radisic et al., 2003; 2008; Vunjak-Novakovic and Radisic, 2004).

On the other hand, the culture medium flow was relatively low in order to guarantee enough nutrients and oxygen supplementation for cell survival and differentiation without suffering due to high shear stress exposure.

The model system used in this study also has some limitations. SM were used as cell source because they provide a well characterized and highly controlled proof-of-principle model for cardiac TE investigation, and due to the well knowledge (Gianni-Barrera et al., 2013; Marsano et al., 2013) and ready availability within the lab. However, for future *in vivo* tests, SMs cannot electrically couple with the resident cardiomyocytes and thus can interfere with cardiac conduction and give rise to arrhythmias (Menasché et al., 2008; Gepstein et al., 2010).

Our results provide proof-of-principle for generating a thick-relevant cardiac SM-based contractile 3D patch to be used as functional substitutes or as biological *in vitro* research model systems. The present study demonstrated that perfusion can markedly and significantly improve the viability, the contractility, and the uniformity of the engineered tissue, allowing cells to express differentiated phenotype. Future work is expected to be driven by the need to create thick-relevant grafts with homogeneous tissue architectures for controlled *in vitro* and *in vivo* studies. In particular, there is a need to co-culture the SMs with a vasculogenic cell source in order to obtain a spatially uniform prevascular network, to compartmentalize nutrient supply and waste removal in a more physiological way, and to enhance cell survival during *in vitro* cultivation and *in vivo* implantation. As possible strategy, mesenchymal progenitor cells from adipose tissue do not cause arrhythmias (Sanchez et al., 2010), are currently undergoing clinical evaluation for the treatment of cardiac ischemia (Perin et al., 2010; Houtgraaf et al., 2012), and we could take advantages from the knowledge of the group about this type of cells (Scherberich et al., 2010; Güven et al., 2011). Moreover, in the next future, the same experiments with a more suitable cell line for cardiac TE, as human cardiac progenitor cells derived by heart auricles biopsies, will be investigated.

5. Conclusions

We report a new approach of cardiac TE to generate reproducible thick-relevant SM-based contractile 3D patches, that is based on the combination of a perfusion-based bioreactor culture system and type I collagen scaffold. After culture in a perfusion-based bioreactor using three different cell culture medium, SM differentiation was induced with a homogeneous distribution within the entire volume of the scaffold, leading to survival of the seeded SMs and significant improvement of cardiac contractility. This study confirmed the critical roles of perfusion stimulation, cell density, and medium composition for the formation of engineered cardiac tissue to be used as functional substitute or as biological *in vitro* research model system.

Acknowledgments

The authors gratefully acknowledge funding of this research provided by Schweizerische Herzstiftung.

References

Al Attar N, Carrion C, Ghostine S, Garcin I, Vilquin JT, Hagège AA, Menasché P. Long-term (1 year) functional and histological results of autologous skeletal muscle cells transplantation in rat. *Cardiovascular Research*, 2003, 58(1):142-8.

Bajaj P, Reddy B Jr, Millet L, Wei C, Zorlutuna P, Bao G, Bashir R. Patterning the differentiation of C2C12 skeletal myoblasts. *Integrative Biology*, 2011, 3(9):897-909.

Beltrami AP, Barlucchi L, Torella D, Baker M, Limana F, Chimenti S, Kasahara H, Rota M, Musso E, Urbanek K, Leri A, Kajstura J, Nadal-Ginard B, Anversa P. Adult cardiac stem cells are multipotent and support myocardial regeneration. *Cell*, 2003, 114(6):763-76.

Birla RK, Huang YC, Dennis RG. Development of a novel bioreactor for the mechanical loading of tissue-engineered heart muscle. *Tissue Engineering*, 2007, 13(9):2239-48.

Blumenthal B, Golsong P, Poppe A, Heilmann C, Schlensak C, Beyersdorf F, Siepe M. Polyurethane scaffolds seeded with genetically engineered skeletal myoblasts: a promising tool to regenerate myocardial function. *Artificial Organs*, 2010, 34(2):E46-54.

Brasselet C, Morichetti MC, Messas E, Carrion C, Bissery A, Bruneval P, Vilquin JT, Lafont A, Hagège AA, Menasché P, Desnos M. Skeletal myoblast transplantation through a catheter-based coronary sinus approach: an effective means of improving function of infarcted myocardium. *European Heart Journal*, 2005, 26(15):1551-6.

Boheler KR, Czyz J, Tweedie D, Yang HT, Anisimov SV, Wobus AM. Differentiation of pluripotent embryonic stem cells into cardiomyocytes. *Circulation Research*, 2002, 91(3):189-201.

Bursac N, Papadaki M, Cohen RJ, Schoen FJ, Eisenberg SR, Carrier R, Vunjak-Novakovic G, Freed LE. Cardiac muscle tissue engineering: toward an in vitro model for electrophysiological studies. *American Journal of Physiology*, 1999, 277(2 Pt 2):H433-44.

Carrier RL, Papadaki M, Rupnick M, Schoen FJ, Bursac N, Langer R, Freed LE, Vunjak-Novakovic G. Cardiac tissue engineering: cell seeding, cultivation parameters, and tissue construct characterization. *Biotechnology and Bioengineering*, 1999, 64(5):580-9.

Carrier RL, Rupnick M, Langer R, Schoen FJ, Freed LE, Vunjak-Novakovic G. Effects of oxygen on engineered cardiac muscle. *Biotechnology and Bioengineering*, 2002a, 78(6):617-25.

Carrier RL, Rupnick M, Langer R, Schoen FJ, Freed LE, Vunjak-Novakovic G. Perfusion improves tissue architecture of engineered cardiac muscle. *Tissue Engineering*, 2002b, 8(2):175-88.

Chiu LLY, Radisic M. 2013. Cardiac tissue engineering. *Current Opinion in Chemical Engineering*, 2013, 2(1):41-52.

Durrani S, Konoplyannikov M, Ashraf M, Haider KH. Skeletal myoblasts for cardiac repair. *Regenerative Medicine*, 2010, 5(6):919-32.

Elliott NT, Yuan F. A review of three-dimensional in vitro tissue models for drug discovery and transport studies. *Journal of Pharmaceutical Sciences*, 2011, 100(1):59-74.

Fink C, Ergün S, Kralisch D, Remmers U, Weil J, Eschenhagen T. Chronic stretch of engineered heart tissue induces hypertrophy and functional improvement. *FASEB Journal*, 2000, 14(5):669-79.

Gepstein L, Ding C, Rahmutula D, Wilson EE, Yankelson L, Caspi O, Gepstein A, Huber I, Olgin JE. In vivo assessment of the electrophysiological integration and arrhythmogenic risk of myocardial cell transplantation strategies. *Stem Cells*, 2010, 28 (12):2151-61.

Ghostine S, Carrion C, Souza LC, Richard P, Bruneval P, Vilquin JT, Pouzet B, Schwartz K, Menasché P, Hagege AA. Long-term efficacy of myoblast transplantation on regional structure and function after myocardial infarction. *Circulation*, 2002, 106(12 Suppl 1):I131-6.

Gianni-Barrera R, Trani M, Fontanellaz C, Heberer M, Djonov V, Hlushchuk R, Banfi A. VEGF over-expression in skeletal muscle induces angiogenesis by intussusception rather than sprouting. *Angiogenesis*, 2013, 16(1):123-36.

Gonen-Wadmany M, Gepstein L, Seliktar D. Controlling the cellular organization of tissue-engineered cardiac constructs. *Annals of the New York Academy of Sciences*, 2004, 1015:299-311.

Goto S, Miyazaki K, Funabiki T, Yasumitsu H. Serum-free culture conditions for analysis of secretory proteinases during myogenic differentiation of mouse C2C12 myoblasts. *Analytical Biochemistry*. 1999 Aug 1;272(2):135-42.

Guo XM, Zhao YS, Chang HX, Wang CY, E LL, Zhang XA, Duan CM, Dong LZ, Jiang H, Li J, Song Y, Yang XJ. Creation of engineered cardiac tissue in vitro from mouse embryonic stem cells. *Circulation*, 2006, 113(18):2229-37.

Güven S, Mehrkens A, Saxer F, Schaefer DJ, Martinetti R, Martin I, Scherberich A. Engineering of large osteogenic grafts with rapid engraftment capacity using mesenchymal and endothelial progenitors from human adipose tissue. *Biomaterials*, 2011, 32(25):5801-9.

Habeler W, Pouillot S, Plancheron A, Pucéat M, Peschanski M, Monville C. An in vitro beating heart model for long-term assessment of experimental therapeutics. *Cardiovascular Research*, 2009, 81(2):253-9.

Haider HKh, Ye L, Jiang S, Ge R, Law PK, Chua T, Wong P, Sim EK. Angiomyogenesis for cardiac repair using human myoblasts as carriers of human vascular endothelial growth factor. *Journal of Molecular Medicine*, 2004, 82(8):539-49.

Hamdi, H.; Planat-Benard, V.; Bel, A.; Puymirat, E.; Geha, R.; Pidial, L.; Nematalla, H.; Bellamy, V.; Bouaziz, P.; Peyrard, S.; Casteilla, L.; Bruneval, P.; Hagege, A. A.; Agbulut, O.; Menasche, P. Epicardial adipose stem cell sheets results in greater post-infarction survival than intramyocardial injections. *Cardiovascular Research*, 2011, 91 (3):483-491.

Hansen A, Eder A, Bönstrup M, Flato M, Mewe M, Schaaf S, Aksehirliglu B, Schwörer A, Uebeler J, Eschenhagen T. Development of a Drug Screening Platform Based on Engineered Heart Tissue. *Circulation Research*, 2010, 107:35-44.

Hata H, Matsumiya G, Miyagawa S, Kondoh H, Kawaguchi N, Matsuura N, Shimizu T, Okano T, Matsuda H, Sawa Y. Grafted skeletal myoblast sheets attenuate myocardial remodeling in pacing-induced canine heart failure model. *The Journal of Thoracic and Cardiovascular Surgery*, 2006, 132(4):918-24.

Hirt MN, Sörensen NA, Bartholdt LM, Boeddinghaus J, Schaaf S, Eder A, Vollert I, Stöhr A, Schulze T, Witten A, Stoll M, Hansen A, Eschenhagen T. Increased afterload induces pathological cardiac hypertrophy: a new in vitro model. *Basic Research in Cardiology*, 2012, 107(6):307.

He KL, Yi GH, Sherman W, Zhou H, Zhang GP, Gu A, Kao R, Haimes HB, Harvey J, Roos E, White D, Taylor DA, Wang J, Burkhoff D. Autologous skeletal myoblast transplantation improved hemodynamics and left ventricular function in chronic heart failure dogs. *The Journal of Heart and Lung Transplantation*, 2005, 24(11):1940-9.

Houtgraaf JH, den Dekker WK, van Dalen BM, Springeling T, de Jong R, van Geuns RJ, Geleijnse ML, Fernandez-Aviles F, Zijlstra F, Serruys PW, Duckers HJ. First experience in humans using adipose tissue-derived regenerative cells in the treatment of patients with ST-segment elevation myocardial infarction. *Journal of the American College of Cardiology*, 2012, 59(5):539-40.

Khan M, Kutala VK, Vikram DS, Wisel S, Chacko SM, Kuppusamy ML, Mohan IK, Zweier JL, Kwiatkowski P, Kuppusamy P. Skeletal myoblasts transplanted in the ischemic myocardium enhance in situ oxygenation and recovery of contractile function. *Heart and Circulatory Physiology - American Journal of Physiology*, 2007, 293(4):H2129-39.

Kim DH, Lipke EA, Kim P, Cheong R, Thompson S, Delannoy M, Suh KY, Tung L, Levchenko A. Nanoscale cues regulate the structure and function of macroscopic cardiac tissue constructs. *Proceedings of the National Academy of Sciences USA*, 2010, 107:565-570.

Kroehne V, Heschel I, Schügner F, Lasrich D, Bartsch JW, Jockusch H. Use of a novel collagen matrix with oriented pore structure for muscle cell differentiation in cell culture and in grafts. *Journal of Cellular and Molecular Medicine*, 2008, 12(5A):1640-8.

Lawson MA, Purslow PP. Differentiation of myoblasts in serum-free media: effects of modified media are cell line-specific. *Cells Tissues Organs*, 2000, 167(2-3):130-7.

Ma J, Holden K, Zhu J, Pan H, Li Y. The application of three-dimensional collagen-scaffolds seeded with myoblasts to repair skeletal muscle defects. *Journal of Biomedicine and Biotechnology*, 2011, 812135.

Maidhof R, Marsano A, Lee EJ, Vunjak-Novakovic G. Perfusion seeding of channeled elastomeric scaffolds with myocytes and endothelial cells for cardiac tissue engineering. *Biotechnology Progress*, 2010, 26(2):565-72.

McCue JD, Swingen C, Feldberg T, Caron G, Kolb A, Denucci C, Prabhu S, Motilall R, Breviu B, Taylor DA. The real estate of myoblast cardiac transplantation: negative remodeling is associated with location. *The Journal of Heart and Lung Transplantation*, 2008, 27(1):116-23.

Menasché P. Skeletal myoblast transplantation for cardiac repair. *Expert Review of Cardiovascular Therapy*, 2004, 2(1):21-8.

Menasché P. Skeletal myoblasts and cardiac repair. *Journal of Molecular and Cellular Cardiology*, 2008, 45(4):545-53.

Marsano A, Maidhof R, Luo J, Fujikara K, Konofagou EE, Banfi A, Vunjak-Novakovic G. The effect of controlled expression of VEGF by transduced myoblasts in a cardiac patch on vascularization in a mouse model of myocardial infarction. *Biomaterials*, 2013, 34(2):393-401.

Martinez-Fernandez A, Nelson TJ, Yamada S, Reyes S, Alekseev AE, Perez-Terzic C, Ikeda Y, Terzic A. iPS programmed without c-MYC yield proficient cardiogenesis for functional heart chimerism. *Circulation Research*, 2009, 105(7):648-56.

Massai D, Cerino G, Gallo D, Pennella F, Deriu MA, Rodriguez A, Montecvecchi FM, Bignardi C, Audenino A, Morbiducci U. Bioreactors as engineering support to treat cardiac muscle and vascular disease. *Journal of Healthcare Engineering*, 2013, 4(3):329-70.

Mauritz C, Schwanke K, Reppel M, Neef S, Katsirntaki K, Maier LS, Nguemo F, Menke S, Hausteiner M, Hescheler J, Hasenfuss G, Martin U. Generation of functional murine cardiac myocytes from induced pluripotent stem cells. *Circulation*, 2008, 118(5):507-17.

Meinel L, Hofmann S, Karageorgiou V, Zichner L, Langer R, Kaplan D, Vunjak-Novakovic G. Engineering cartilage-like tissue using human mesenchymal stem cells and silk protein scaffolds. *Biotechnology and Bioengineering*, 2004a, 88:379–391.

Meinel L, Karageorgiou V, Hofmann S, Fajardo R, Snyder B, Li C, Zichner L, Langer R, Vunjak-Novakovic G, Kaplan DL. Engineering bone-like tissue in vitro using human bone marrow stem cells and silk scaffolds. *Journal of Biomedical Materials Research Part A*, 2004b, 71:25–34.

Mummery C, Ward D, van den Brink CE, Bird SD, Doevendans PA, Opthof T, Brutel de la Riviere A, Tertoolen L, van der Heyden M, Pera M. Cardiomyocyte differentiation of mouse and human embryonic stem cells. *Journal of Anatomy*, 2002, 200(Pt 3):233-42.

Narazaki G, Uosaki H, Teranishi M, Okita K, Kim B, Matsuoka S, Yamanaka S, Yamashita JK. Directed and systematic differentiation of cardiovascular cells from mouse induced pluripotent stem cells. *Circulation*, 2008, 118(5):498-506.

Orlic D, Kajstura J, Chimenti S, Jakoniuk I, Anderson SM, Li B, Pickel J, McKay R, Nadal-Ginard B, Bodine DM, Leri A, Anversa P. Bone marrow cells regenerate infarcted myocardium. *Nature*, 2001, 410(6829):701-5.

Perin EC, Sanchez PL, Ruiz RS, Perez-Cano R, Lasso J, Alonso-Farto JC, Fernandez-Pina L, Serruys PW, Duckers HJ (Eric), Kastrup J, Chameleau S, Zheng Y, Silva GV, Milstein AM, Martin MT, Willerson JT, Aviles FF. First in man transendocardial injection of autologous AdiPose-deRived StEm cells in patients with non Revascularizable Ischemic myocardium (PRECISE). *Circulation*, 2010, 122.

Planat-Benard V, C. Menard, M. Andre, M. Puceat, A. Perez, J.M. Garcia-Verdugo, L. Penicaud, L. Casteilla. Spontaneous cardiomyocyte differentiation from adipose tissue stroma cells. *Circulation Research*, 2004, 94:223–229

Portiér GL, Benders AG, Oosterhof A, Veerkamp JH, van Kuppevelt TH. Differentiation markers of mouse C2C12 and rat L6 myogenic cell lines and the effect of the differentiation medium. *In Vitro Cellular & Developmental Biology - Animal*, 1999, 35(4):219-27.

Radisic M, Euloth M, Yang L, Langer R, Freed LE, Vunjak-Novakovic G. High-density seeding of myocyte cells for cardiac tissue engineering. *Biotechnology and Bioengineering*, 2003, 82(4):403-14.

Radisic M, Park H, Shing H, Consi T, Schoen FJ, Langer R, Freed LE, Vunjak-Novakovic G. Functional assembly of engineered myocardium by electrical stimulation of cardiac myocytes cultured on scaffolds. *Proceedings of the National Academy of Sciences USA*, 2004, 101(52):18129-34.

Radisic M, Marsano A, Maidhof R, Wang Y, Vunjak-Novakovic G. Cardiac tissue engineering using perfusion bioreactor systems. *Nature Protocols*, 2008, 3(4):719-38.

Rando TA, Blau HM. Primary mouse myoblast purification, characterization, and transplantation for cell-mediated gene therapy. *The Journal of Cell Biology*, 1994, 125:1275–1287.

Ravichandran R, Venugopal JR, Sundarrajan S, Mukherjee S, Sridhar R, Ramakrishna S. Expression of cardiac proteins in neonatal cardiomyocytes on PGS/fibrinogen core/shell substrate for Cardiac tissue engineering. *International Journal of Cardiology*, 2013, 167(4):1461-8.

Sanchez PL, Sanz-Ruiz R, Fernandez-Santos ME, Fernandez-Aviles F. Cultured and freshly isolated adipose tissue-derived cells: fat years for cardiac stem cell therapy. *European Heart Journal*, 2010, 31(4):394-7.

Scherberich A, Galli R, Jaquier C, Farhadi J, Martin I. Three-dimensional perfusion culture of human adipose tissue-derived endothelial and osteoblastic progenitors generates osteogenic constructs with intrinsic vascularization capacity. *Stem Cells*, 2007, 25(7):1823-9.

Scherberich A, Müller AM, Schäfer DJ, Banfi A, Martin I. Adipose tissue-derived progenitors for engineering osteogenic and vasculogenic grafts. *Journal of Cellular Physiology*, 2010, 225(2):348-53.

Siepe M, Giraud MN, Liljensten E, Nydegger U, Menasché P, Carrel T, Tevaearai HT. Construction of skeletal myoblast-based polyurethane scaffolds for myocardial repair. *Artificial Organs*, 2007, 31(6):425-433.

Smits AM, van Vliet P, Metz CH, Korfage T, Sluijter JP, Doevendans PA, Goumans MJ. Human cardiomyocyte progenitor cells differentiate into functional mature cardiomyocytes: an in vitro model for studying human cardiac physiology and pathophysiology. *Nature Protocols*, 2009, 4(2):232-43.

Sun Y, Ge Y, Drnevich J, Zhao Y, Band M, Chen J. Mammalian target of rapamycin regulates miRNA-1 and follistatin in skeletal myogenesis. *The journal of cell biology*, 2010, 28;189(7):1157-69.

Tandon N, Cannizzaro C, Chao PH, Maidhof R, Marsano A, Au HT, Radisic M, Vunjak-Novakovic G. Electrical stimulation systems for cardiac tissue engineering. *Nature Protocols*, 2009, 4(2):155-73.

Taylor DA, Atkins BZ, Hungspreugs P, Jones TR, Reedy MC, Hutcheson KA, Glower DD, Kraus WE. Regenerating functional myocardium: improved performance after skeletal myoblast transplantation. *Nature Medicine*, 1998, 4(8):929-33.

von Wattenwyl R, Blumenthal B, Heilmann C, Golsong P, Poppe A, Beyersdorf F, Siepe M. Scaffold-based transplantation of vascular endothelial growth factor-overexpressing stem cells leads to neovascularization in ischemic myocardium but did not show a functional regenerative effect. *ASAIO Journal*, 2012, 58(3):268-74.

Vunjak-Novakovic G, Radisic M. Cell seeding of polymer scaffolds. *Methods in Molecular Biology*, 2004, 238:131-46.

Vunjak-Novakovic G, Tandon N, Godier A, Maidhof R, Marsano A, Martens TP, Radisic M. Challenges in cardiac tissue engineering. *Tissue Engineering Part B Reviews*, 2010, 16(2):169-87.

Wendt D, Marsano A, Jakob M, Heberer M, Martin I. Oscillating perfusion of cell suspensions through three-dimensional scaffolds enhances cell seeding efficiency and uniformity. *Biotechnology and Bioengineering*, 2003, 84(2):205-14.

Ye L, Haider HKh, Jiang S, Ling LH, Ge R, Law PK, Sim EK. 2005. Reversal of myocardial injury using genetically modulated human skeletal myoblasts in a rodent cryoinjured heart model. *European Journal of Heart Failure*, 2005, 7(6):945-52.

Ye L, Haider HKh, Jiang S, Tan RS, Ge R, Law PK, Sim EK. Improved angiogenic response in pig heart following ischaemic injury using human skeletal myoblast simultaneously expressing VEGF165 and angiopoietin-1. *European Journal of Heart Failure*, 2007, 9(1):15-22.

Yoshiko Y, Hirao K, Maeda N. Differentiation in C2C12 myoblasts depends on the expression of endogenous IGFs and not serum depletion. *American Journal of Physiology - Cell Physiology*, 2002, 283:C1273-C1286.

Zheng H, Liu S, Tian W, Yan H, Zhang Y, Li Y. A three-dimensional in vitro culture model for primary neonatal rat ventricular myocytes. *Current Applied Physics*, 2012, 12(3): 826-833.

Zhou YF, Sae-Lim V, Chou AM, Hutmacher DW, Lim TM. Does seeding density affect in vitro mineral nodules formation in novel composite scaffolds? *Journal of Biomedical Materials Research Part A*, 2006, 78(1):183-93.

Zimmermann WH, Didié M, Wasmeier GH, Nixdorff U, Hess A, Melnychenko I, Boy O, Neuhuber WL, Weyand M, Eschenhagen T. Cardiac grafting of engineered heart tissue in syngenic rats. *Circulation*, 2002a, 106(12 Suppl 1):I151-7.

Zimmermann WH, Schneiderbanger K, Schubert P, Didié M, Münzel F, Heubach JF, Kostin S, Neuhuber WL, Eschenhagen T. Tissue engineering of a differentiated cardiac muscle construct. *Circulation Research*, 2002b, 90(2):223-30.

Zimmermann WH, Eschenhagen T. Embryonic stem cells for cardiac muscle engineering. Trends in Cardiovascular Medicine, 2007, 17(4):134-40.

Zwi-Dantsis L, Mizrahi I, Arbel G, Gepstein A, Gepstein L. Scalable production of cardiomyocytes derived from c-Myc free induced pluripotent stem cells. Tissue Engineering Part A, 2011, 17(7-8):1027-37.

CHAPTER V

Conclusions and Future Works

1. Summary and conclusions

It is evident that there are increasing efforts in developing *in vitro* strategies and methods for assessing fundamental myocardial biology and physiology. In addition, recently, there is an increasing interest in generation of engineered cardiac constructs *in vitro* to repair damaged tissues *in vivo*. Therefore, finding innovative approaches for developing engineered cardiac constructs will be a major focus of future work in cardiac tissue engineering (TE). Thus, future studies will address the issue of how to design cell-scaffold-bioreactor systems to be used as three-dimensional (3D) model systems for investigating the developmental aspects of tissue maturation, and the influence of different biophysical stimuli and mass transport on tissue formation, structure, and function.

In this framework, the works presented in this thesis demonstrate that a comprehensive approach, combining complementary aspects of cardiac TE as bioreactor-based technologies and biological strategies, could provide innovative support tools that will be of practical use in the near future, as improved experimental models, and as model systems for cardiac development, representing, in the late future, an effective therapeutic strategy to the reestablishment of the structure and function of injured cardiac tissues in the clinical practice.

The objectives of this thesis, based on engineering and biological approaches in the field of cardiac TE, can be summarized as follow:

- 1) development of two dedicated bioreactors for cardiac TE, and in detail
 - optimization and implementation of a bioreactor for culturing cell-seeded cardiac patches, designed for generating a physiological biochemical and physical environment that mimics the native stimuli of the cardiac tissue, by providing uniaxial cyclic stretching and electrical stimulations;
 - design of an innovative and low-cost suspension bioreactor that, due to its peculiar geometric features, allows the formation of buoyant vortices that guarantee the establishment of suspension and low-shear cell culture conditions within the culture chamber, without using electromechanical rotating systems;
- 2) engineering of reproducible thick-relevant skeletal myoblast (SM)-based contractile 3D patches by using perfusion-based bioreactor culture system and type I collagen scaffold.

The combination of bioreactor culture systems dedicated to cardiac TE and biological cardiac substitutes, that mimic the cardiac natural extracellular matrix (ECM), could represent an effective model system for investigating the still unknown mechanisms of cardiac development and for drug screening based on the effects of pharmacological compounds on biological tissues, and a physiological model of human disease processes

that might be prevented or treated if better understood. Moreover, in the late future, such approach could represent an effective therapeutic strategy to the reestablishment of the structure and function of injured cardiac tissues in the clinical practice.

The principal contributions from each chapter of this thesis are summarized below.

Chapter I – Introduction

The introductory chapter provides a general overview of the anatomy and pathologies of the human heart, and a literature review of the cardiac TE background that was necessary to understand and guide the work of this thesis.

Chapter II – An electro-mechanical bioreactor providing physiological-like cardiac stimuli.

With the intent to overcome the limitations of the current available bioreactor systems for providing physiological-like cardiac stimuli, as the inability to delivery mechanical and electrical stimuli at the same time, and to satisfy the good laboratory practice (GLP) rules, in this chapter we have presented the optimization and the implementation of a previously developed electro-mechanical bioreactor for culturing cell-seeded cardiac patches, designed for generating a physiological biochemical and physical environment that mimics the native stimuli of the cardiac tissue, by providing uniaxial cyclic stretching and electrical stimulations. Our results demonstrated as the bioreactor optimizations performed, allowed to obtain a multipurpose adaptable system for dynamic culture of cell-seeded scaffolds, that can be used as a model system for 1) testing cytocompatibility and durability of seeded patches, and 2) investigating the influence of electro-mechanical stimulation on cells cultured on patches. Preliminary findings suggest that in the next future this bioreactor could also be used as a production system for implantable functional engineered constructs.

Chapter III – An innovative suspension bioreactor.

Suspension culture methods are the most popular means for preventing problems related to the two-dimensional (2D) cell culture conditions, by providing a suitable biochemical and hydrodynamic 3D environment in the effort to replicate the physical and structural components of the native-like microenvironments. In this chapter we have provided an alternative solution for recreating suspension conditions, developing an innovative and low-cost bioreactor that, due to the peculiar geometric features, assures the generation of buoyant vortices and the consequent establishment of suspension conditions without using electromechanical rotating systems. This behavior allows the creation of a biochemical and

hydrodynamic environment suitable 1) to maintain specimens of different dimensions in suspension conditions, 2) to guarantee suitable oxygen and nutrient transport, and 3) to avoid critical shear stress values affecting the cells by guaranteeing laminar flow conditions. Our findings demonstrated as the bioreactor developed presents the potentiality to be used as a model system 1) for testing cell/cell-microsphere constructs cytocompatibility and durability, and 2) for investigating the influence of suspension condition on cells cultured with or without microspheres. Preliminary findings suggest that in the next future this bioreactor could also be used as an expansion, aggregation and differentiation system for *in vitro* cell culture.

Chapter IV – Generation of contractile 3D muscle-like tissue in a perfusion-based bioreactor culture system.

Cardiac TE has shown the potential to generate thick-contractile myocardium-like constructs that might be used as functional substitutes or as biological *in vitro* model systems to investigate the cardiac tissue-specific development and diseases, and to offer accurate and controlled *in vitro* tests for cell and cardiac tissue-based therapies, drug screening, predictive toxicology and target validation. Within this scenario, with the aim to provide an innovative biological *in vitro* model system for cardiac TE investigations, we have engineered reproducible thick-relevant SM-based contractile 3D patches by using perfusion-based bioreactor culture system and type I collagen scaffold. Our results provided proof-of-principle for generating a thick-relevant cardiac SM-based contractile 3D patch, demonstrating that perfusion can markedly and significantly improve the viability, the contractility, and the uniformity of the engineered tissue, allowing cells to express differentiated phenotype.

2. Limitations

Notwithstanding their consistency, the approaches developed within this thesis present some limitations:

1) *Lack of a real-time monitoring and control system.* In works presented in Chapter II and III, one of the major important limitations of the bioreactors developed is the lack of a real-time monitoring system of both culture operating conditions and construct development.

In this context, besides monitoring the milieu parameters (e.g.: temperature, pressure, flow rate, pH, dissolved oxygen and carbon dioxide, metabolite/catabolite concentrations, sterility, etc.), monitoring function and structure (e.g.: stiffness, force, strength, permeability, composition of the scaffold, cell number, cell viability, etc.) of developing engineered cardiac constructs, and design minimally invasive yet reliable

monitoring techniques still remain relatively unexplored areas and a highly challenging fields of research (Wendt et al., 2009). To date, many real-time monitoring methods are available for bioreactors, including conventional electrochemical sensors, and non-invasive spectroscopic and optical technologies (Beutel and Henkel, 2011; Teixeira et al., 2011). Integration of real-time monitoring technologies should minimize the amount of sample extracted for analysis and any disruption to the cell culture itself. Alternatively *in-situ* probes may be incorporated into the bioreactor and this is one of the most favored designs.

In Chapter II the development of a sensing control block responsible for real-time signal acquisition and display without interrupt the cellular experiment is briefly presented. At present, only strain signal is available, but this block has been designed to be modular and ready to be used for pH, temperature, partial pressure of oxygen signal acquisition and display. The user-friendly software for both control and acquisition will allow the user to easily perform three types of control over the bioreactor: 1) mechanical stimulation only, 2) real-time sensing only and 3) mechanical stimulation and real-time sensing. This findings is in line with the current literature studies, in fact, although contractile function is one of the most important outputs of engineered cardiac tissues, only a few existing platforms are equipped with systems for quantitative force measurement. Some authors transfer the generated tissue from a cultivation vessel to a measurement device or organ bath chamber (Eschenhagen et al., 1997; 2002; Fink et al., 2000; Zimmermann et al., 2000; 2002; 2006; Radisc et al., 2003). A possible weakness of such approach is that force measurement is predominantly used as an end-point analysis, and several samples are needed for long-term data acquisitions, entailing a huge amount of cells needed, more than that for continuous analyses. Recently developed miniaturized platforms attempt to bridge this gap by allowing direct (using specific force sensors (Kensah et al., 2011)) or indirect (using optical analysis (Hansen et al., 2010; Boudou et al., 2012)) measurement of the contraction forces, providing noninvasive online monitoring during prolonged culture.

In Chapter III the possibility to implement specific sensors and control system for the on-line, high throughput monitoring of basic parameters such as temperature, pH, partial pressure of oxygen and carbon dioxide is under investigation. These functioning modalities will be suitable for a lot of experiments aimed at investigated the environment within the culture chamber, providing the user with several quantitative data to be used to implement a control system of the experimental parameters.

2) *Cell source*. In work presented in Chapter IV one of the major important limitations of the engineered cardiac patch developed concerns the choice of an unsuitable cell source for cardiac TE.

SMs are widely use in cardiac TE thanks to their high proliferative potential, high resistance to ischemia, and their fate restriction to the myogenic lineage, with the capacity to develop a complete contractile apparatus, virtually eliminates the risk of tumorigenicity

(Manasché, 2004; 2008). On the other hand, the major disadvantage of SMs is that they do not electrically couple with the host cardiomyocytes (Durrani et al., 2010), and this obviously raises the major question of the mechanisms by which, in case of cell transplantation, the myoblasts can improve left ventricular function (Manasché, 2004).

Despite this concern, within this work, SMs were used as cell source because they provide a well characterized and highly controlled proof-of-principle model for cardiac TE investigation, and due to the well knowledge (Gianni-Barrera et al., 2013; Marsano et al., 2013) and ready availability within the lab.

3. Recommendations for future works

For overcoming the above mentioned limitations, in the future further in-depth strategies could be developed in order to:

- 1) integrate real-time monitoring technologies for minimizing the amount of sample extracted for analysis and any disruption to the cell culture itself, by incorporating *in-situ* probe, conventional electrochemical sensors, and non-invasive spectroscopic and optical technologies;
- 2) simplify the process for minimizing the operator dependent variability, the labor costs, and the time and effort needed in order to perform experiments, by reducing the number of the bioreactor variables/components, therefore making easier the use of the systems also by non-experienced staff;
- 3) perform experiments in a condition much closer to the native-like environment, by changing the cell source with a more suitable cell line for cardiac TE, as human cardiac progenitor cells derived by heart auricles biopsies.

Moreover, a further study could concern the creation of thick-relevant grafts with homogeneous tissue architectures for controlled *in vitro* and studies. In particular, there is a need to co-culture the cardiac cells with a vasculogenic cell source in order to obtain a spatially uniform prevascular network, to compartmentalize nutrient supply and waste removal in a more physiological way, and to enhance cell survival during *in vitro* cultivation and *in vivo* implantation. As possible strategy, cell-based angiogenic approaches focused on the use of not genetically modified mesenchymal stem cells (MSC) of different origins, are becoming promising strategy for supporting the regeneration of injured cardiac tissues (Melly et al., 2012). Specifically, adipose tissue-derived stromal vascular fraction (SVF) are currently undergoing clinical evaluation for the treatment of cardiac ischemia (Perin et al., 2010; Houtgraaf et al., 2012), and contain a heterogeneous cell population, which makes SVF cells capable of both *in vitro* and *in vivo* vasculogenesis.

Furthermore, due to the importance that the topic is having in the last decade within the scientific community, a further line of research could consist in the exploration of the role of bioreactors in the stem cell (SC) culture. Currently, in fact, the large majority

of SC products undergoing translation into the clinic, particularly those to be used in regenerative medicine settings, rely on traditional static culture systems to achieve required cell doses. However, the successful implementation of SC therapies requires the large-scale production of SC products, regulated by industrial manufacturing standards with proven reproducibility and process quality control. The recent advances in the development of bioreactor systems for the expansion of SC and/or their controlled differentiation have now taken this technology to the point where clinical-scale productivities can be achieved. In addition, the success of clinical trials involving SC and the necessary approval of these therapies by regulatory agencies will demand more advanced and cost-effective manufacturing tools. The translation of bioreactor systems, with integrated and customized downstream processing, to good manufacturing practice (GMP) conditions will be very important for the large-scale production of SC therapies. In addition, although most clinical trials are currently being or will be run using SC produced using classic, static culture systems, these systems can later be replaced by bioreactor systems when required for market-scale production, if such systems are approved by regulatory agencies through drug comparability studies (e.g. to assure product identity, therapeutic potency and safety). It will then be critical to continue the development of bioreactors for SC expansion, under GMP-guided research, to overcome the expected technological barriers that will likely be encountered when these therapies reach the market stage (dos Santos et al., 2013).

References

Beutel S, Henkel S. In situ sensor techniques in modern bioprocess monitoring. *Applied Microbiology and Biotechnology*, 2011, 91(6):1493-505.

Boudou T, Legant WR, Mu A, Borochin MA, Thavandiran N, Radisic M, Zandstra PW, Epstein JA, Margulies KB, Chen CS. A microfabricated platform to measure and manipulate the mechanics of engineered cardiac microtissues. *Tissue Engineering Part A*, 2012, 18(9–10):910–919.

dos Santos FF, Andrade PZ, da Silva CL, Cabral JM. Bioreactor design for clinical-grade expansion of stem cells. *Biotechnology Journal*, 2013, 8(6):644-54.

Durrani S, Konoplyannikov M, Ashraf M, Haider KH. Skeletal myoblasts for cardiac repair. *Regenerative Medicine*, 2010, 5(6):919-32.

Eschenhagen T, Fink C, Remmers U, Schols H, Wattchow J, Weil J, Zimmermann W, Dohmen HH, Schäfer H, Bishopric N, Wakatsuki T, Elson EL. Three dimensional reconstitution of embryonic cardiomyocytes in a collagen matrix: a new heart muscle model system. *Federation of American Societies for Experimental Biology Journal*, 1997, 11:683–694.

Eschenhagen T, Didié M, Heubach J, Ravens U, Zimmerman WH. Cardiac tissue engineering. *Transplant Immunology*, 2002, 9(2–4):315–321.

Fink C, Ergün S, Kralisch D, Remmers U, Weil J, Eschenhagen T. Chronic stretch of engineered heart tissue induces hypertrophy and functional improvement. *Federation of American Societies for Experimental Biology Journal*, 2000, 14(5):669–679.

Gianni-Barrera R, Trani M, Fontanellaz C, Heberer M, Djonov V, Hlushchuk R, Banfi A. VEGF over-expression in skeletal muscle induces angiogenesis by intussusception rather than sprouting. *Angiogenesis*, 2013, 16(1):123-36.

Hansen A, Eder A, Bönstrup M, Flato M, Mewe M, Schaaf S, Aksehirliglu B, Schwörer A, Uebeler J, Eschenhagen T. Development of a Drug Screening Platform Based on Engineered Heart Tissue. *Circulation Research*, 2010, 107:35–44.

Houtgraaf JH, den Dekker WK, van Dalen BM, Springeling T, de Jong R, van Geuns RJ, Geleijnse ML, Fernandez-Aviles F, Zijlstra F, Serruys PW, Duckers HJ. First experience in humans using adipose tissue-derived regenerative cells in the treatment of patients with ST-

segment elevation myocardial infarction. *Journal of the American College of Cardiology*, 2012, 59(5):539-40.

Kensah G, Gruh I, Viering J, Schumann H, Dahlmann J, Meyer H, Skvorc D, Bär A, Akhyari P, Heisterkamp A, Haverich A, Martin U. A novel miniaturized multimodal bioreactor for continuous in situ assessment of bioartificial cardiac tissue during stimulation and maturation. *Tissue Engineering Part C Methods*, 2011, 17(4):463–473.

Marsano A, Maidhof R, Luo J, Fujikara K, Konofagou EE, Banfi A, Vunjak-Novakovic G. The effect of controlled expression of VEGF by transduced myoblasts in a cardiac patch on vascularization in a mouse model of myocardial infarction. *Biomaterials*, 2013, 34(2):393-401.

Melly L, Boccardo S, Eckstein F, Banfi A, Marsano A. Cell and Gene Therapy Approaches for Cardiac Vascularization. *Cells*, 2012, 1(4):961-975.

Menasché P. Skeletal myoblast transplantation for cardiac repair. *Expert Review of Cardiovascular Therapy*, 2004, 2(1):21-8.

Menasché P. Skeletal myoblasts and cardiac repair. *Journal of Molecular and Cellular Cardiology*, 2008, 45(4):545-53.

Perin EC, Sanchez PL, Ruiz RS, Perez-Cano R, Lasso J, Alonso-Farto JC, Fernandez-Pina L, Serruys PW, Duckers HJ (Eric), Kastrup J, Chameleau S, Zheng Y, Silva GV, Milstein AM, Martin MT, Willerson JT, Aviles FF. First in man transendocardial injection of autologous AdiPose-derived StEm cells in patients with non Revascularizable Ischemic myocardium (PRECISE). *Circulation*, 2010, 122.

Radisic M, Euloth M, Yang L, Langer R, Freed LE, Vunjak-Novakovic G. High-density seeding of myocyte cells for cardiac tissue engineering. *Biotechnology and Bioengineering*, 2003, 82(4):403–414.

Teixeira AP, Duarte TM, Carrondo MJ, Alves PM. Synchronous fluorescence spectroscopy as a novel tool to enable PAT applications in bioprocesses. *Biotechnology and Bioengineering*, 2011, 108(8):1852-61.

Wendt D, Riboldi SA, Cioffi M, Martin I. Potential and bottlenecks of bioreactors in 3D cell culture and tissue manufacturing. *Advanced Materials*, 2009, 21(32–33):3352–3367.

Zimmermann WH, Fink C, Kralisch D, Remmers U, Weil J, Eschenhagen T. Three-dimensional engineered heart tissue from neonatal rat cardiac myocytes. *Biotechnology and Bioengineering*, 2000, 68(1):106–114.

Zimmermann WH, Didié M, Wasmeier GH, Nixdorff U, Hess A, Melnychenko I, Boy O, Neuhuber WL, Weyand M, Eschenhagen T. Cardiac grafting of engineered heart tissue in syngenic rats. *Circulation*, 2002, 106(12 Suppl 1):151–157.

Zimmermann WH, Melnychenko I, Wasmeier G, Didié M, Naito H, Nixdorff U, Hess A, Budinsky L, Brune K, Michaelis B, Dhein S, Schwoerer A, Ehmke H, Eschenhagen T. Engineered heart tissue grafts improve systolic and diastolic function in infarcted rat hearts. *Nature Medicine*, 2006, 12(4):452–458.

